AGU PUBLICATIONS

Water Resources Research

RESEARCH ARTICLE
10.1002/2014WR015617

Key Points:
- A photon budget approach was used to analyze underwater light in a reservoir
- Transparency was controlled by dissolved organic matter not by phytoplankton
- This limits application of traditional water quality descriptors (Secchi depth)

Supporting Information:
- Supporting Information S1

Correspondence to:
S. Watanabe,
swata213@gmail.com

Citation:
Watanabe, S., I. Laurion, S. Markager, and W. F. Vincent (2015), Abiotic control of underwater light in a drinking water reservoir: Photon budget analysis and implications for water quality monitoring, *Water Resour. Res.*, *51*, 6290–6310, doi:10.1002/2014WR015617.

Received 22 MAR 2014
Accepted 1 JUL 2015
Accepted article online 4 JUL 2015
Published online 14 AUG 2015

Abiotic control of underwater light in a drinking water reservoir: Photon budget analysis and implications for water quality monitoring

Shohei Watanabe[1,2,3], Isabelle Laurion[3,4], Stiig Markager[5], and Warwick F. Vincent[1,3]

[1]Département de Biologie, Université Laval, Québec City, Québec, Canada, [2]Now at Tahoe Environmental Research Center, University of California, Davis, California, USA, [3]Centre d'études nordiques (CEN: Centre for Northern Studies), Université Laval, Québec City, Québec, Canada, [4]Institut national de la recherche scientifique, Centre Eau Terre Environnement, Québec City, Québec, Canada, [5]Department of Bioscience, Aarhus University, Roskilde, Denmark

Abstract In optically complex inland waters, the underwater attenuation of photosynthetically active radiation (PAR) is controlled by a variable combination of absorption and scattering components of the lake or river water. Here we applied a photon budget approach to identify the main optical components affecting PAR attenuation in Lake St. Charles, a drinking water reservoir for Québec City, Canada. This analysis showed the dominant role of colored dissolved organic matter (CDOM) absorption (average of 44% of total absorption during the sampling period), but with large changes over depth in the absolute and relative contribution of the individual absorption components (water, nonalgal particulates, phytoplankton and CDOM) to PAR attenuation. This pronounced vertical variation occurred because of the large spectral changes in the light field with depth, and it strongly affected the average *in situ* diffuse absorption coefficients in the water column. For example, the diffuse absorption coefficient for pure-water in the ambient light field was 10-fold higher than the value previously measured in the blue open ocean and erroneously applied to lakes and coastal waters. Photon absorption budget calculations for a range of limnological conditions confirmed that phytoplankton had little direct influence on underwater light, even at chlorophyll *a* values above those observed during harmful algal blooms in the lake. These results imply that traditional measures of water quality such as Secchi depth and radiometric transparency do not provide a meaningful estimate of the biological state of the water column in CDOM-colored lakes and reservoirs.

1. Introduction

In the blue waters of the open ocean, the variability of underwater light attenuation is controlled by phytoplankton and other covarying optical components. Sea surface color therefore provides a quantitative guide to oceanic phytoplankton stocks, and this is the basis of remote sensing techniques for estimating algal concentrations [*International Ocean Color Coordinating Group (IOCCG)* 2000]. Similarly, water transparency measurements, including Secchi disk measurements, have been used as a guide to changes in phytoplankton biomass and primary production in the world ocean [*Boyce et al.*, 2010]. In contrast, the underwater light field in lakes, reservoirs and coastal systems is often governed by several noncovarying optical components: colored dissolved organic matter (CDOM), algal particles, nonalgal particles (NAP) encompassing both organic and inorganic particulate materials, as well as the water itself. Many of these vary independently, and the optical conditions of freshwater and coastal waters are considerably more complex than in open oceans [*Bukata*, 2005].

Two classes of variables describe the optical properties of natural waters: apparent optical properties (AOPs), which are dependent both on the characteristics of the water and the ambient light field, and inherent optical properties (IOPs), which are inherent to the medium and independent of the ambient irradiance field [*Kirk*, 1994; *Mobley*, 1994]. An AOP of major ecological and geophysical significance is $K_d(PAR)$, the diffuse attenuation coefficient for downward irradiance (E_d) in the photosynthetically active radiation waveband (PAR; 400–700 nm; the notation for all variables is given in Table 1). This is used to define the depth of the euphotic zone for phytoplankton, the depth limit of macrophytes [*Markager and Sand-Jensen*, 1992; *Middelboe and Markager*, 1997], as well as the availability of light for visual predators and photobiological processes [*Kalff*, 2002; *Kirk*, 1994]. $K_d(PAR)$ is also a key parameter in heat budget calculations [*Morel and Antoine*, 1994; *Patterson and Hamblin*, 1988], and correlates with Secchi depth [*Koenings and Edmundson*, 1991;

Table 1. Notation Used in this Article

Symbol	Variable and Unit
λ	wavelength, nm
z	depth, m
Chl a	chlorophyll *a* concentration, μg Chl *a* L^{-1}
SPM_i	Suspended particulate matter (i=total (T), inorganic (I) or organic (O)), mg L^{-1}
DOC	dissolved organic carbon, mg carbon L^{-1}
$E_d(z;\lambda)$	spectral downward irradiance, W m^{-2} nm^{-1}
$E_{q;d}(z;\lambda)$	spectral downward photon flux density, μmol m^{-2} nm^{-1} s^{-1}
$K_d(\lambda)$	spectral diffuse attenuation coefficient of downward photon flux density, m^{-1}
$K_d(PAR)$	diffuse attenuation coefficient for photosynthetically active radiation (PAR) in the euphotic zone depth, m^{-1}
$K_d(z;PAR)$	diffuse attenuation coefficient for PAR at depth z, m^{-1}
$a_i(\lambda)$	absorption coefficient of component i, m^{-1}
$a_i^*(\lambda)$	mass-specific absorption coefficient of component i
S_i	exponential slope parameter of component i.
$c_{t-w}(\lambda)$	beam attenuation coefficient excluding effects of pure-water for unfiltered water samples, m^{-1}
$b_p(\lambda)$	scattering coefficient of suspended particulate matter, m^{-1}
$b_p^*(\lambda)$	SPM_T-specific scattering coefficient of suspended particulate matter, m^2 SMP g^{-1}
$b_t/a_t(\lambda)$	ratio of total scattering to total absorption coefficient, dimensionless
$\overline{\mu}_d(z;\lambda)$	average cosine for downward irradiance, dimensionless
$a_{D;i}(z;\lambda)$	diffuse absorption coefficient of optical component i for downward irradiance, m^{-1}
$K_d'(z;PAR)$	estimated diffuse attenuation coefficient for PAR at depth z, m^{-1}
	z_{ave} = averaged over euphotic zone
	z_{eu} = at the bottom of euphotic zone

Preisendorfer, 1986], which is among the most commonly measured parameters for water quality monitoring in lakes and reservoirs [e.g., *Dodson*, 2005; *Kalff*, 2002].

$K_d(PAR)$ can be partitioned into components associated with each of the optical components of the water column [*Kirk*, 1994; *Mobley*, 1994; *Murray et al*., 2015], and such an analysis provides information on the controlling variables for underwater light transmission. These component-specific attenuation coefficients are typically estimated by conducting multiple linear regressions on data obtained under a wide range of optical conditions [e.g., *Carstensen et al*., 2013; *Duarte et al*., 1998; *Balogh et al*., 2009]. An alternative approach, termed the photon budget calculation, is based on a spectral analysis of combined AOP and IOP measurements, and was introduced by *Smith et al*. [1989] to partition the effects of different optical components on PAR attenuation in the open ocean. However, there has been little subsequent application of this approach [*Giles-Guzman and Alvarez-Borrego*, 2000].

Lake St. Charles (46°56′ N, 71°23′ W) is a reservoir located 20 km north of Québec City, Québec, Canada (Figure 1) [*Tremblay et al*., 2001] that supplies drinking water to 285,000 residents. It has a surface area of 3.6 km^2 and a catchment area of 166 km^2 that has extensive areas of mixed broadleaf-conifer forest (80%) but also with developed urban areas (13%). The mean water residence time in summer is 72 days [*Pienitz and Vincent*, 2003; *Tremblay et al*., 2001]. It is a dimictic lake with anoxic conditions in its deepest waters in late summer [*Rolland et al*., 2013]. The lake is subject to ongoing eutrophication, and the recent appearance of toxic cyanobacterial blooms is an issue of major public concern [*Rolland and Vincent*, 2014].

In the present study, we applied a photon budget analysis to Lake St. Charles. Our aims were to determine how the optical components of lake water affected the vertical distribution of underwater light, and to separate their individual contributions to spectral attenuation as a function of depth. We measured downward spectral irradiance throughout the summer months, and combined these data with laboratory measurements of IOPs and other limnological variables. We also determined how the dominant PAR absorbing components varied in relative importance over a potential range of limnological conditions in the lake, and evaluated the implications for water quality measurements based on transparency.

2. Methods

2.1. Sampling

Lake St. Charles was sampled on 10 June 2008, and biweekly from 8 July to 30 September 2008 (n = 8) at the deepest point (16.6 m) located in the north basin. Sampling was always conducted within 3 h of local solar noon. Surface water (50 cm below the surface) was taken with Nalgene amber polyethylene bottles

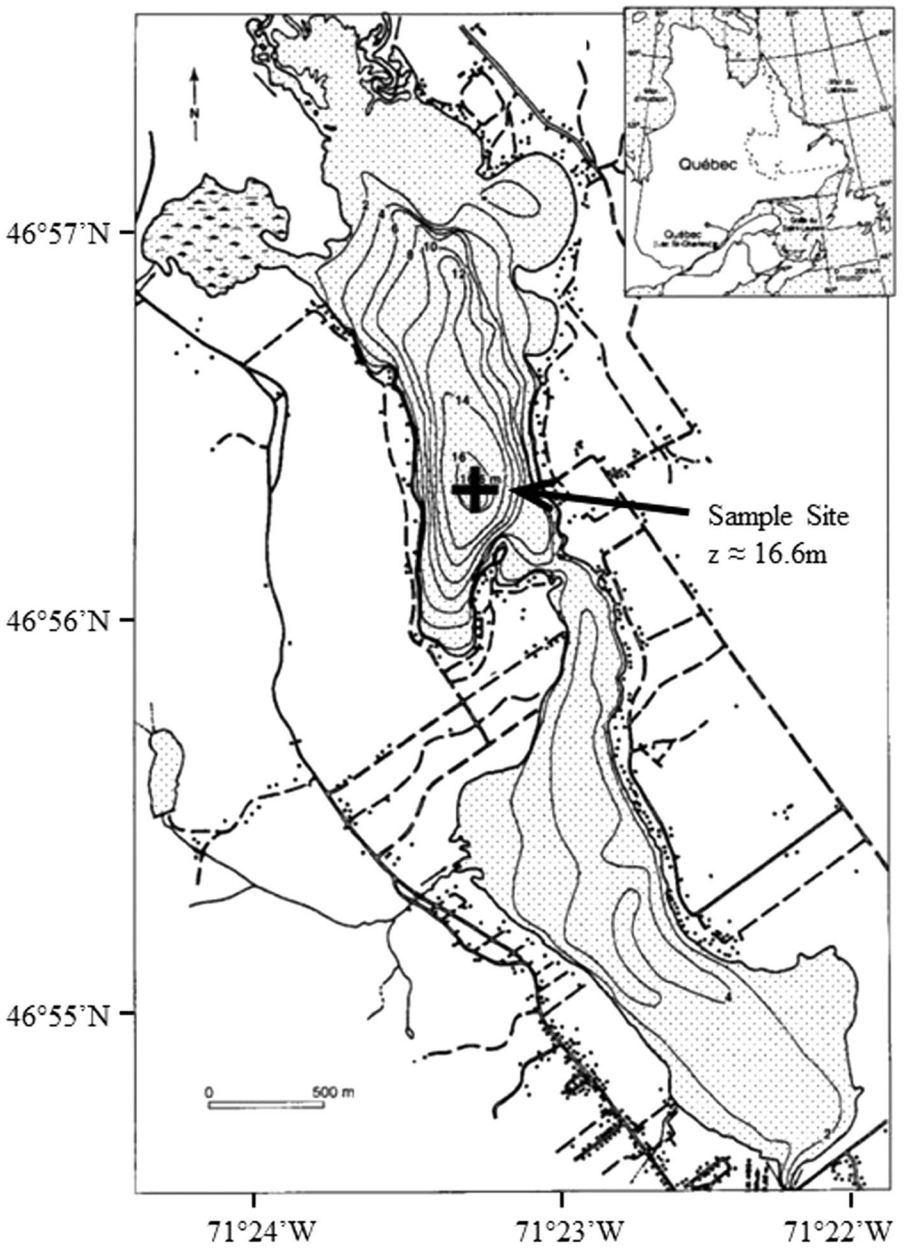

Figure 1. Map showing the location and bathymetry of Lake St. Charles, modified from *Tremblay et al.* [2001]. The sample site is indicated as a cross.

(Thermo Fisher Scientific Inc., USA) and kept refrigerated in the dark until processing in the laboratory within 5 h of collection [*APHA*, 1998].

2.2. Radiometric Measurements and Apparent Optical Properties

The vertical profiles of spectral downward irradiance ($E_d(z;\lambda)$, W m^{-2} nm^{-1}) were obtained with a hyperspectral radiometer system (HyperPro, Satlantic Inc., Canada), consisting of two HyperOCRs (hyperspectral downward irradiance and upward radiance sensors) and a Profiler II (controlling unit with temperature and pressure sensors). The instrument was manually lowered on the side of the boat facing the sun at approximately 5 cm s^{-1}, and the instrument was kept away from the boat to avoid shadow effects while profiling. The instrument regularly measured shutter dark values during the profiling and a dark correction was applied in the subsequent data processing. Raw data were processed to radiometric values by the manufacturer provided software (ProSoft Version 7.7.15, Satlantic Inc., Canada). The radiometric data were linearly

interpolated to obtain the spectral profiles of $E_d(z;\lambda)$ from 352 to 797 nm at 1 nm intervals, and averaged at 10 cm depth intervals. For the subsequent data analyses, $E_d(z;\lambda)$ values were converted to the spectral downward photon flux density ($E_{q;d}(z;\lambda)$, μmol m^{-2} nm^{-1} s^{-1}) as:

$$E_{q;d}(z;\lambda) = \frac{E_d(z;\lambda)\cdot\lambda}{h\cdot c\cdot N_A}\times 10^6 \quad (1)$$

where h is Planck's constant, c the speed of light, and N_A is Avogadro's number. The vertical profiles of downward photon flux density for PAR ($E_{q;d}(z;PAR)$, μmol m^{-2} s^{-1}) were then obtained by summing $E_{q;d}(z;\lambda)$ over the range 400 to 700 nm.

Three different diffuse attenuation coefficients were calculated. The spectral diffuse attenuation coefficients of downward photon flux density ($K_d(\lambda)$, m^{-1}) were obtained by regressing $E_{q;d}(z;\lambda)$ over the depth range from just below the surface to the depth where $E_{q;d}(z;\lambda)$ reached 1% of the surface value. Similarly, the diffuse attenuation coefficient for PAR in the euphotic zone depth ($K_d(PAR)$, m^{-1}) was calculated for $E_{q;d}(z;PAR)$ from the surface to the limit of the euphotic zone, where $E_{q;d}(z;PAR)$ reached 1% of the surface value. The diffuse attenuation coefficient for PAR at depth z ($K_d(z;PAR)$, m^{-1}) was calculated by regressing $E_{q;d}(z;PAR)$ over a depth range of 1 m centered at z; for example, the coefficient at 2 m depth ($K_d(2;PAR)$) was calculated using the 11 values of $E_{q;d}(z;PAR)$ from 1.5 to 2.5 m.

2.3. Laboratory Analyses of Limnological Variables

Water samples were filtered through GF/F glass fiber filters (25 mm diameter, 0.7 μm pore size, Whatman Inc., USA) and the filters were stored frozen (−80°C) for less than 6 months until laboratory analysis for chlorophyll *a* concentrations (Chl *a*, μg L^{-1}). Pigments were extracted in ethanol and Chl *a* concentration was determined by fluorometry (Cary Eclipse spectrofluorometer, Varian Inc., Canada) before and after acidification [*Nusch*, 1980]. Water samples were also filtered onto precombusted and preweighed GF/F filters (47 mm diameter) to quantify suspended particulate matter. Filters were weighed after drying for 2 h at 60°C to determine total suspended particulate matter (SPM_T, mg L^{-1}). Subsequently, filters were combusted at 500°C for 2 h, and then reweighed to estimate inorganic suspended particulate matter (SPM_I, mg L^{-1}). Organic suspended particulate matter (SPM_O, mg L^{-1}) estimates were obtained as the difference between SPM_T and SPM_I [*Breton et al*., 2009]. Dissolved organic carbon (DOC, mg L^{-1}) concentrations were measured with a TOC-5000A carbon analyzer (Shimadzu Co., Japan) calibrated with potassium biphthalate [*Breton et al*., 2009]. Water samples were filtered through cellulose acetate filters (47 mm diameter, 0.2 μm pore size, Advantec MFS Inc., USA) that were prerinsed by pure water prepared with an EASY pure II UV/UF system (Barnstead International, USA), and the filtrate was stored in the dark at 4°C for up to 2 weeks until analysis.

2.4. Inherent Optical Properties

For analysis of colored dissolved organic matter (CDOM), water samples were filtered through GF/F filters (47 mm diameter) and subsequently through the nitrocellulose membrane filters (47 mm diameter), and the filtrates were refrigerated in amber glass bottles until analysis. The absorbance ($A(\lambda)$, dimensionless) of the filtrate against pure-water was measured from 200 to 850 nm at 1 nm intervals (spectral slit width 2 nm) in a 1 cm quartz cuvette using a Cary 100 dual beam spectrophotometer (Varian Inc., Canada). The absorption coefficients of CDOM ($a_{CDOM}(\lambda)$, m^{-1}) were calculated as:

$$a_{CDOM}(\lambda) = \frac{2.303A(\lambda)}{L} \quad (2)$$

where L is the path length of the cuvette. Null point correction was conducted by subtracting the average of $a_{CDOM}(\lambda)$ from 750 to 760 nm where the absorption curves became flat [*Mitchell et al*., 2002; *Mitchell et al*., 2000]. The exponential slope parameters of the spectra (S_{CDOM}) were calculated by nonlinearly fitting the measured value from 300 to 650 nm to the equation:

$$a_{CDOM}(\lambda) = a_{CDOM}(\lambda_0)\cdot e^{-S_{CDOM}(\lambda-\lambda_0)} \quad (3)$$

where λ_0 is the reference wavelength as 440 nm [*Bricaud et al*., 1981; *Stedmon et al*., 2000]. The DOC-specific absorption coefficient of CDOM ($a_{CDOM}^*(\lambda)$, m^2 g^{-1}C) was calculated as $a_{CDOM}(\lambda)$ divided by DOC concentration.

Suspended particles in the lake water were filtered onto GF/F filters (25 mm diameter) and stored up to 10 months at −80°C until optical analysis. Absorbance of this particulate matter was measured by the wet filter technique (quantitative filter technique) in the same spectrophotometer as above equipped with an integrating sphere, with the filter held by a sample holder at the entrance of the sphere (Labsphere Inc., USA) following *Mitchell et al*. [2002]. The absorbance of nonalgal particles was then measured by the same technique after extracting pigments from the filter sample with methanol [*Kishino et al*., 1985; *Mitchell et al*., 2002]. The optimal depigmentation protocol for particle samples from inland waters is a subject of ongoing discussion [*Binding et al*., 2008]; in the present study, the widely applied methanol extraction method was sufficient to remove algal pigments, and no absorption peaks of remnant pigments were observed after extraction. The absorption coefficients of total and nonalgal particulate matter ($a_p(\lambda)$ and $a_{NAP}(\lambda)$ in m^{-1}, respectively) were calculated as:

$$a_p(\lambda) \text{ or } a_{NAP}(\lambda) = \frac{2.303A(\lambda) \cdot T}{\beta \cdot V} \quad (4)$$

where T is the filtered area, V is filtered volume, and β is the path length amplification factor [*Mitchell et al*., 2002]. A constant value for $\beta = 2$ was used after *Roesler* [1998]. There have been several methods suggested for the beta estimation [*Cleveland and Weidemann*, 1993; *Mitchell et al*., 2002], and this remains a source of uncertainty. Comparison of the absorption coefficient spectra obtained with this constant beta with those obtained with the method of *Bricaud and Stramski* [1990], also widely used, gave root mean square differences in the range 0.02 to 0.05 m^{-1}. Thus the uncertainty associated with the beta factor may be considered minor. Null point correction was applied in the same manner as for $a_{CDOM}(\lambda)$. The absorption coefficient of algal particles ($a_\Phi(\lambda)$, m^{-1}) was obtained by subtracting $a_{NAP}(\lambda)$ from $a_p(\lambda)$. Similar to $a_{CDOM}(\lambda)$, the exponential slope parameter of the $a_{NAP}(\lambda)$ spectra (S_{NAP}) was calculated by fitting equation (3) to the data. Nonlinear regression was conducted over the spectral range 380–730 nm excluding the ranges 400–480 and 620–710 nm to eliminate the residual pigment absorption [*Babin et al*., 2003a; *Belzile et al*., 2004]. The SPM_T-specific absorption coefficient of nonalgal particulate matter ($a_{NAP}^*(\lambda)$, $m^2\ g^{-1}$ SPM) and Chl *a*-specific absorption coefficient of algal particles ($a_\Phi^*(\lambda)$, $m^2\ mg^{-1}$ Chl *a*) were also calculated.

The GF/F filtrate was filtered onto nitrocellulose membrane filters (25 mm diameter, 0.2 μm pore size; Millipore Co., USA) and the absorption coefficient of materials collected on the filters (fine particles, $a_{fine}(\lambda)$, m^{-1}) was determined using the same method as for the $a_p(\lambda)$ quantification described above, and similar to methods applied elsewhere [e.g., *Ferrari and Tassan*, 1996] including for fine particles [*Gallegos*, 2005; *Watanabe et al*., 2011]. A major source of uncertainty for such analysis is the beta factor for nitrocellulose membrane filters, which likely differs from that of glass fiber filters. Full evaluation of this method, for example by the approach of *Babin and Stramski* [2002], is needed for future studies of fine particle optics.

2.5. Blank and Duplicate Preparation

Blanks and duplicates were prepared for each sampling event to check the precision of the laboratory analyses. Blanks were prepared for SPM, DOC, $a_{CDOM}(\lambda)$, and $a_p(\lambda)$ using pure water (as above) that was treated in the same way as the samples. These blanks were then analyzed as the natural water samples and the obtained values, if above the detection limit (which was rarely the case), were subtracted from lake water samples for correction. For Chl *a*, SPM, $a_{CDOM}(\lambda)$, and $a_p(\lambda)$, duplicate samples were analyzed and the averaged values were used for subsequent data analyses. The average differences between duplicates were 11% (SPM_T), 10% (Chl *a*), 5% ($a_{CDOM}(440)$), and 3% ($a_p(440)$).

2.6. AC-S Measurement

The absorption and beam attenuation coefficients for unfiltered water samples ($a_{t-w}(\lambda)$ and $c_{t-w}(\lambda)$ in m^{-1}, respectively) were measured using an AC-S spectrophotometer (25 cm path length, WET Labs Inc., USA) mounted on the laboratory bench [*Watanabe et al*., 2011]. Pure-water calibration values obtained immediately before the sampling period were subtracted from the raw readings and a temperature correction was applied by using the spectral correction coefficients obtained specifically for our instrument [*Pegau et al*., 2003; *Sullivan et al*., 2006; *Twardowski et al*., 1999]. A null point correction was applied by subtracting the absorption coefficient at the longest wavelength measured by the instrument (751.7 nm), as in *Pegau et al*. [2003].

The measured spectral ranges of our instrument were 403.0–751.7 nm for $a_{t-w}(\lambda)$ and 401.6–750.8 nm for $c_{t-w}(\lambda)$. The resultant spectra were linearly interpolated for the range 403–700 nm at 1 nm intervals to align

with other IOPs and for summation over the PAR range for the photon budget calculations (see equation (7)). The spectra were extrapolated to 400 nm by fitting the measured values from 403 to 410 nm to the exponential model as in equation (3). This extrapolation of $c_{t-w}(\lambda)$ spectra was considered appropriate because of the high contribution of CDOM absorption and relatively minor contribution of scattering over this wavelength range (mean contribution of $b_p(403)$ in $c_{t-w}(403)$ was 28%). The scattering coefficients of suspended particulate matter ($b_p(\lambda)$, m^{-1}) were then obtained by subtracting $a_{t-w}(\lambda)$ from $c_{t-w}(\lambda)$. The SPM_T-specific scattering coefficients for suspended particulate matter ($b_p^*(\lambda)$, $m^2\ g^{-1}$) were obtained by dividing $b_p(\lambda)$ by SPM_T. Finally, the total absorption coefficient ($a_t(\lambda)$, m^{-1}) was obtained by adding the absorption coefficient of pure-water ($a_w(\lambda)$, m^{-1}) [*Pope and Fry*, 1997] to the $a_{t-w}(\lambda)$ values, and the total scattering coefficient ($b_t(\lambda)$, m^{-1}) was obtained by adding the scattering coefficient of pure-water $b_w(\lambda)$ [*Buiteveld et al*., 1994] to the $b_p(\lambda)$ values.

2.7. Photon Budget Calculations

The classic work by *Preisendorfer* [1961, 1976] showed that the diffuse attenuation coefficient of $E_d(z;\lambda)$ can be calculated as:

$$K_d(z;\lambda) = a_D(z;\lambda) + b_{b;D}(z;\lambda) - b_{b;D;u}(z;\lambda)\cdot R(z;\lambda) \tag{5}$$

where $a_D(z;\lambda)$ is the diffuse absorption coefficient for downward irradiance, $b_{b;D}(z;\lambda)$ is the diffuse backscattering coefficient for downward irradiance, $b_{b;D;u}(z;\lambda)$ is the diffuse backscattering coefficient for upward irradiance, and $R(z;\lambda)$ is the irradiance reflectance, defined as the ratio of upward irradiance to downward irradiance. Theoretically, $a_D(z;\lambda)$ can be subdivided into the optical components due to the additive nature of the absorption coefficient. The $b_{b;D;u}(z;\lambda)\cdot R(z;\lambda)$, representing downward scattering of upward irradiance, should be negligible relative to $a_D(z;\lambda)$ and $b_{b;D}(z;\lambda)$ in water bodies where the ratio of scattering to absorption is low (1% at b/a = 3) [*Kirk*, 1981] and can be ommited from the equation [*Smith et al*., 1989]. Thus, the diffuse attenuation coefficient of downward irradiance can be estimated as:

$$K_d(z;\lambda) = \sum_{i=1}^{n} a_{D;i}(z;\lambda) + b_{b;D}(z;\lambda) \tag{6}$$

where $a_{D;i}(z;\lambda)$ is the diffuse absorption coefficient of optical component *i*. The conceptual background to this $K_d(z;\lambda)$ approximation from IOPs have been discussed in detail by *Smith et al*. [1989] and *Kirk* [1994].

In the present study, four absorbing components measured by laboratory spectrophotometry (CDOM, NAP, algal particles, and fine particles) and pure-water [*Pope and Fry*, 1997] were considered, and their absorption spectra were applied for the subsequent calculations. The backscattering coefficient ($b_b(\lambda)$, m^{-1}) was estimated by multiplying $b_p(\lambda)$ by the backscattering ratio of 0.018 [*Petzold*, 1972]. The contributions of chlorophyll fluorescence and bioluminescence to photon budgets in the open ocean have been shown to be orders of magnitude lower than other optical components [*Smith et al*., 1989]; these contributions were therefore assumed to be negligible in the present study, also since the absorption and scattering coefficients for Lake St. Charles were much higher than for the offshore ocean.

The inherent optical properties of each optical component were measured with collimated light, and were therefore converted to the diffuse absorption and backscattering coefficients of downward radiation ($a_{D;i}(z;\lambda)$ and $b_{b;D}(z;\lambda)$, respectively) by dividing with the average cosine of downward irradiance ($\overline{\mu}_d(z;\lambda)$, dimensionless), the ratio of the downward irradiance to the downward scalar irradiance [*Kirk*, 1994]. The parameter $\overline{\mu}_d(z;\lambda)$ was assumed constant with a value of 0.8 [*Smith et al*., 1989]. These diffuse absorption oefficients were subsequently incorporated into the spectrally weighted diffuse absorption coefficient of component *i* for PAR ($a_{D;i}(z;PAR)$) as:

$$a_{D;i}(z;PAR) = \frac{\int_{400}^{700} a_{D;i}(z;\lambda)\cdot E_{q;d}(z;\lambda)d\lambda}{\int_{400}^{700} E_{q;d}(z;\lambda)d\lambda} \tag{7}$$

The spectrally weighted diffuse backscattering coefficient for PAR ($b_{b;D}(z;PAR)$) was calculated in an analogous manner. Finally, the estimated diffuse attenuation coefficient for PAR ($K_d'(z;PAR)$) was calculated as:

$$K_d'(z;PAR) = \sum_{i=1}^{5} a_{D;i}(z;PAR) + b_{b;D}(z;PAR) \quad (8)$$

This estimation was conducted from the surface (0 m) to 6 m at 0.1 m intervals, because the observed bottom of euphotic zone of the study site was always less than 6 m (mean: 4.4 m, see below) during summer. The component-specific absorption and scattering spectra were assumed to be constant throughout the water column.

The $\overline{\mu}_d(z;\lambda)$ value represents the average angular distribution of downward photon flux at a point in the water column [*Kirk*, 1994], and although a constant value of 0.8 was applied in the present study, theoretical studies have shown that there may be spectral and vertical variations. These variations depend on factors such as the scattering to absorption ratio, scattering phase function, optical depth, and solar angle [*Berwald et al*., 1995; *Kirk*, 1981], and can be a source of error in estimating component specific diffuse attenuation coefficients [*Stavn*, 1988]. To determine the effect of variations in $\overline{\mu}_d(z;\lambda)$, we applied the HydroLight radiative transfer model (Seqoia Scientific Inc., USA) to estimate this AOP for Lake St. Charles, with the input of lake location, sample time, measured above–water spectral irradiance, $a_{t-w}(\lambda)$ and $c_{t-w}(\lambda)$ measured by AC-S, a backscattering ratio of 0.018, and sky conditions for each sampling day. The resultant $K_d'(z;PAR)$ based on the model prediction of $\overline{\mu}_d(z;\lambda)$ was compared to that calculated with a constant $\overline{\mu}_d(z;\lambda)$ of 0.8, and the difference ranged from -5 to $+6$% for the entire water column throughout the summer. This implies that $\overline{\mu}_d(z;\lambda)$ can be reasonably approximated with a constant value of 0.8 for oligo to mesotrophic waters with relatively low b/a ratios, if measured or estimated values are not available.

The backscattering ratio was assumed to be constant (0.018) [*Petzold*, 1972] in the present study. This value, however, can vary widely depending on particle composition [*Boss et al*., 2004; *Loisel et al*., 2007], and the variation can substantially influence the underwater light field in optically complex inland waters [*Gallegos et al*., 2008; *Peng et al*., 2009]. We estimated the backscattering coefficient from field radiometric measurements by a method based on Monte Carlo simulation ($b_b(\lambda) = a(\lambda)\cdot L_u(\lambda)/0.082\ E_d(\lambda)$, as in *Kirk* [1994]), and this gave values from 0.011 to 0.032 for Lake St. Charles. This three-fold variation in backscattering ratio, however, resulted in only a 3% change in $K_d'(z;PAR)$, and the application of a constant value appears to be appropriate for Lake St. Charles and similar lakes with high total absorption coefficients.

2.8. Photon Absorption Budget Calculations

The fraction of PAR absorbed by each component in the water column was simulated for a range of limnological conditions to further understand the dominant factors controlling PAR attenuation, which is of direct relevance to water quality monitoring and management. The absorption spectrum of each optical component was estimated from the concentration of the respective limnological variable. The absorption spectra of CDOM were estimated from DOC concentrations by estimating absorption at the reference wavelength of 440 nm $a_{CDOM}(440)$ from a regression model (see below), and the $a_{CDOM}(\lambda)$ spectra were estimated from $a_{CDOM}(440)$ by fitting to equation (3). The S_{CDOM} was assumed to be constant, and the summer average value of 0.0157 nm^{-1} (see below) was applied. Similarly, $a_{NAP}(\lambda)$ was estimated from SPM_T concentrations and the exponential model (equation (3)). The summer average (0.0101) of S_{NAP} was applied as the exponential slope, and $a_{NAP}(440)$ was also estimated from SPM_T by a regression model (see below). The $a_\Phi(\lambda)$ spectra were estimated from Chl *a* concentrations by regression models between Chl *a* and $a_\Phi(\lambda)$ for each wavelength. The parameter $a_{fine}(\lambda)$ was assumed to vary within the range of observed values, and for the simulations we used the measured spectra from when $a_{fine}(440)$ was at its minimum (10 June) and maximum (30 September), as well as the average spectrum during the summer. The concentration of optical components was limited to the observed range (DOC: 2.5–4.2 mg L^{-1}, SPM_T: 1.1–2.9 mg L^{-1}) except for Chl *a* concentrations which were extended to 50 μg L^{-1} to simulate extreme algal bloom conditions. The above-water surface irradiance ($E_{q;d}(0^+;\lambda)$) obtained on 19 September was used for all calculations. This spectrum represented the irradiance spectra under a clear sky. All spectra were calculated at 1 nm intervals over the range 400–700 nm. The proportional absorption of photons by each component *i* for PAR was then calculated as:

Table 2. Limnological Conditions of Lake St. Charles in Summer 2008: Chlorophyll *a* (Chl *a*), Dissolved Organic Carbon (DOC), Total Suspended Particulate Matter (SPM_T), Inorganic Suspended Particulate Matter (SPM_I), and Organic Suspended Particulate Matter (SPM_O)[a]

Variables	units	Range	Mean	CV (%)
Chl *a*	$\mu g\ L^{-1}$	3.0–15.4	8.1	53
DOC	$mg\ L^{-1}$	2.5–4.2	3.4	16
SPM_T[b]	$mg\ L^{-1}$	1.1–2.9	2.1	29
SPM_I[b]	$mg\ L^{-1}$	0.2–1.2	0.9	33
SPM_O[b]	$mg\ L^{-1}$	0.8–1.7	1.2	30

[a]CV = coefficient of variation (standard deviation as percentage of the mean).
[b]Data from 8 June 2008 were missing (n = 7).

$$\%a_i(PAR) = \frac{\int_{400}^{700} a_i(\lambda)\cdot E_{q;d}(0^+;\lambda)d\lambda}{\sum_{i=1}^{4}\int_{400}^{700} a_i(\lambda)\cdot E_{q;d}(0^+;\lambda)d\lambda}\times 100 \quad (9)$$

All statistical analyses and model calculations were conducted in R [*R Development Core Team*, 2013].

3. Results

3.1. Limnological Variables

Limnological data for Lake St. Charles over the sampling period are given in Table 2. Chlorophyll *a* concentrations varied by a factor of 5, with higher values in late July and August (9.5–15.4 $\mu g\ L^{-1}$) and low to moderate values (3.0–7.4 $\mu g\ L^{-1}$) for the rest of the summer. This is within the mesotrophic range (10–30 μg Chl *a* L^{-1}) [*MDDEP*, 2007]. SPM_T varied more than two-fold, with no obvious trend during summer. The percent contribution of SPM_I to SPM_T varied from 18 to 52% (mean: 40%), consequently SPM_O accounted for on average 60% of SPM_T but on 3 September 2008 up to 82%. DOC concentrations varied to a lesser extent than SPM and Chl *a*, increasing from 2.5 $mg\ L^{-1}$ (10 June) to 4.2 $mg\ L^{-1}$ (8 July), and then gradually decreasing to 3.1 $mg\ L^{-1}$ on 30 September 2008. The Pearson's product moment correlation analysis showed that there was no significant correlation between DOC and Chl *a* ($r = 0.59$, $p = 0.13$) nor between SPM_T and Chl *a* ($r = 0.51$, $p = 0.24$), however DOC and SPM_T were correlated ($r = 0.78$, $p = 0.04$). Surface water temperature was relatively stable early to mid-summer, varying in range from 18.6 to 22.3°C, and fell to approximately 14.5°C in late summer (19 and 30 September). The water column was stratified approximately at 2 m for the first four observations (10 June to 5 August). The surface mixed layer then deepened to 6 m by late summer. Secchi depth during the period June–September 2008 averaged 2.5 m, with a CV of 16% [*Bourget*, 2011].

3.2. Underwater Irradiance and Apparent Optical Properties

As illustrated by the underwater irradiance spectra on 19 September 2008 (Figure 2), $E_{q;d}(z;\lambda)$ was attenuated more rapidly at shorter relative to longer wavelengths, and similar spectral characteristics were observed throughout the summer. The $K_d(\lambda)$ values were highest at the blue end of the spectrum and lower at the red end (Figure 3). The average $K_d(440)$ was 3.56 m^{-1} with the range 2.52–4.63 m^{-1} (CV: 20%), and the average $K_d(680)$ was 0.95 m^{-1} with a range of 0.79–1.07 m^{-1} (CV: 9%). The lowest $K_d(PAR)$ value (0.77 m^{-1}) was in early summer (10 June); the values increased to a maximum of 1.29 m^{-1} on 8 July, and gradually decreased thereafter to 1.01 m^{-1} during the rest of the summer. Optical depth ($1/K_d(PAR)$) ranged from 0.8 to 1.3 m, and the depth limit of the euphotic zone (1% of surface irradiance) ranged from 3.6 to 6.0 m, with a mean of 4.4 m (CV: 17%).

3.3. Inherent Optical Properties

$a_{CDOM}(440)$ values showed a two-fold variation (Figure 4a and Table 3). The lowest $a_{CDOM}(440)$ value (1.38 m^{-1}) was observed at the beginning of the summer (10 June). The value increased to a maximum of 2.65 m^{-1} one month later (8 July), and then gradually decreased throughout the summer to 1.80 m^{-1}, with a summer average of 2.16 m^{-1}. Although the $a_{CDOM}{}^*(440)$ showed a similar seasonal trend as $a_{CDOM}(440)$, the variation was small (Table 3) and there was a strong linear relationship between CDOM absorption and DOC (Figure 5a). A linear regression analysis showed that there was no significant difference between the intercept and zero; the subsequent regression through the origin gave the model: $a_{CDOM}(440) = 0.63[DOC]$ ($r^2 = 0.92$, $p < 0.01$). S_{CDOM} showed little variation (CV: 1%) with a mean of 0.0157 nm^{-1} throughout the season.

Similar to $a_{CDOM}(440)$, the $a_{NAP}(440)$ values also showed a two-fold variation (Figure 4b and Table 3), but no clear seasonal trend. The specific values, $a_{NAP}{}^*(440)$, ranged from 0.190 to 0.259 $m^2\ g^{-1}$ with a mean of 0.219 $m^2\ g^{-1}$. The mean value of S_{NAP} was 0.010 nm^{-1}, with little variation (Table 3). The $a_{NAP}(440)$ was significantly correlated with both SPM_T ($r = 0.94$, $p < 0.01$) and SPM_I ($r = 0.81$, $p = 0.02$). The relationship between

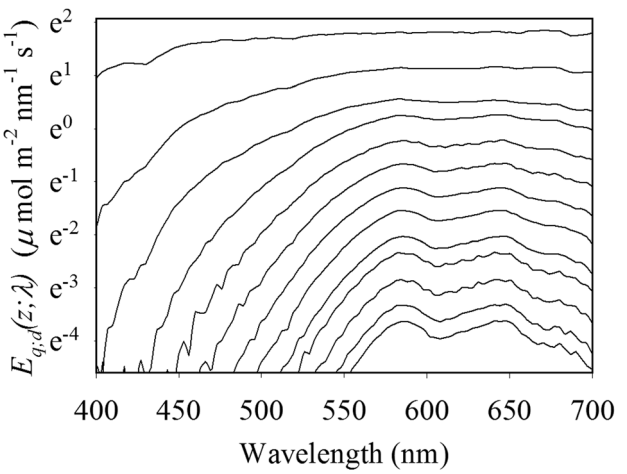

Figure 2. Spectral downward photon flux densities ($E_{q;d}(z;\lambda)$) measured in Lake St. Charles on 19 September 2008. The spectra are from just below the surface (uppermost curve) to 6.0 m at 0.5 m intervals.

$a_{NAP}(440)$ and SPM_T was linearly modeled as $a_{NAP}(440) = 0.21$ [SPM_T] (n = 7, $r^2 = 0.71$, $p < 0.01$, regression through the origin due to no significant intercept, Figure 5b). Values of $a_\Phi(440)$ averaged 0.119 m^{-1} (Figure 4c and Table 3) and varied by a factor of two as a linear function of Chl *a* ($a_\Phi(440) = 0.0064$ [Chl *a*] + 0.0667; $r^2 = 0.85$, $p < 0.01$, intercept significant, Figure 5c). The range of $a_\Phi^*(440)$ was from 0.010 to 0.025 m^2 mg^{-1} Chl *a* (CV: 32%). The absorption of fine particles showed three-fold variation with a mean value of 0.26 m^{-1} (Table 3) and no clear seasonal trend.

The scattering coefficient $b_p(440)$ showed a two-fold variation (Table 3) and was significantly correlated with SPM_T ($r = 0.99$, $p < 0.01$); as a consequence, the specific values for this parameter ($b_p^*(440)$), showed little variation (Table 3). The shape of $b_p(\lambda)$ spectra is often described by a hyperbolic model [*Babin et al.*, 2003a; *Belzile et al.*, 2004]. However, the scattering spectra obtained for Lake St. Charles particles did not fit this model due to inflections in the spectra at the phytoplankton pigment absorption maxima. The ratio of the total scattering to the total absorption coefficient ($b_t/a_t(\lambda)$, dimensionless) showed a two-fold seasonal variation. The spectra displayed peaks at about 585 and 640 nm (Figure 4f). The average value for $b_t/a_t(585)$ was 2.36, with a range from 1.57 to 2.88 (CV: 19%).

3.4. Photon Budget Analyses

On all dates of sampling, the estimated diffuse attenuation coefficient for PAR ($K_d'(z;PAR)$) decreased with depth (Figure 6). On average, $K_d'(z;PAR)$ decreased by 54% from the surface to the bottom of the euphotic zone (range 49–58%). Comparison of $K_d'(z;PAR)$ values estimated from the photon budget calculations with those derived from regressions of measured *in situ* irradiance versus depth in the euphotic zone gave an R^2 of 0.50 (n = 181), with 71% of the values within the RMSE of ±0.19 m^{-1} around the 1:1 line (Figure 7a). The largest deviations were near the surface where large fluctuations were observed in $E_d(z;\lambda)$ due to wave motion, while the values near the bottom of the euphotic zone closely converged. As a further comparison, we also estimated $E_{q;d}(z;PAR)$ from measured photon flux density and the modeled attenuation coefficients as:

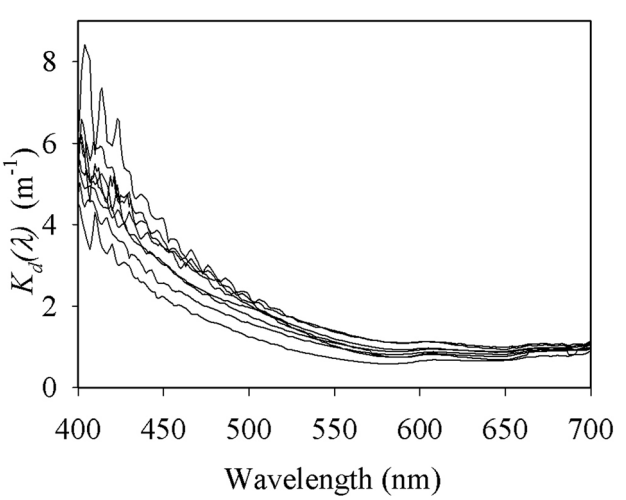

Figure 3. The spectral diffuse attenuation coefficient of downward photon flux density ($K_d(\lambda)$). Observations are shown for all dates of sampling (n = 8).

$$E_{q;d}(z;PAR) = E_{q;d}(z_0;PAR) \cdot e^{-K_d'(z_0;PAR)\cdot(z_0-z)} \quad (10)$$

where z_0 is the depth 0.1m above *z* m (i.e., $z_0 = z - 0.1$). For example, the value at 1 m ($E_{q;d}'(1;PAR)$) was modeled from the measured photon flux density for PAR at 0.9 m ($E_{q;d}(0.9;PAR)$) and modeled attenuation coefficient for PAR at 0.9 m ($K'_d(0.9;PAR)$). When the values were compared with the measured $E_{q;d}(z;PAR)$, the mean absolute percent error was 6% and R^2 was 0.95 in the euphotic zone (n = 334). There was no obvious vertical trend in the error (Figure 7b), except for near surface values showing larger discrepancies due mainly to measurement variations in $E_{q;d}(z;PAR)$ as noted above.

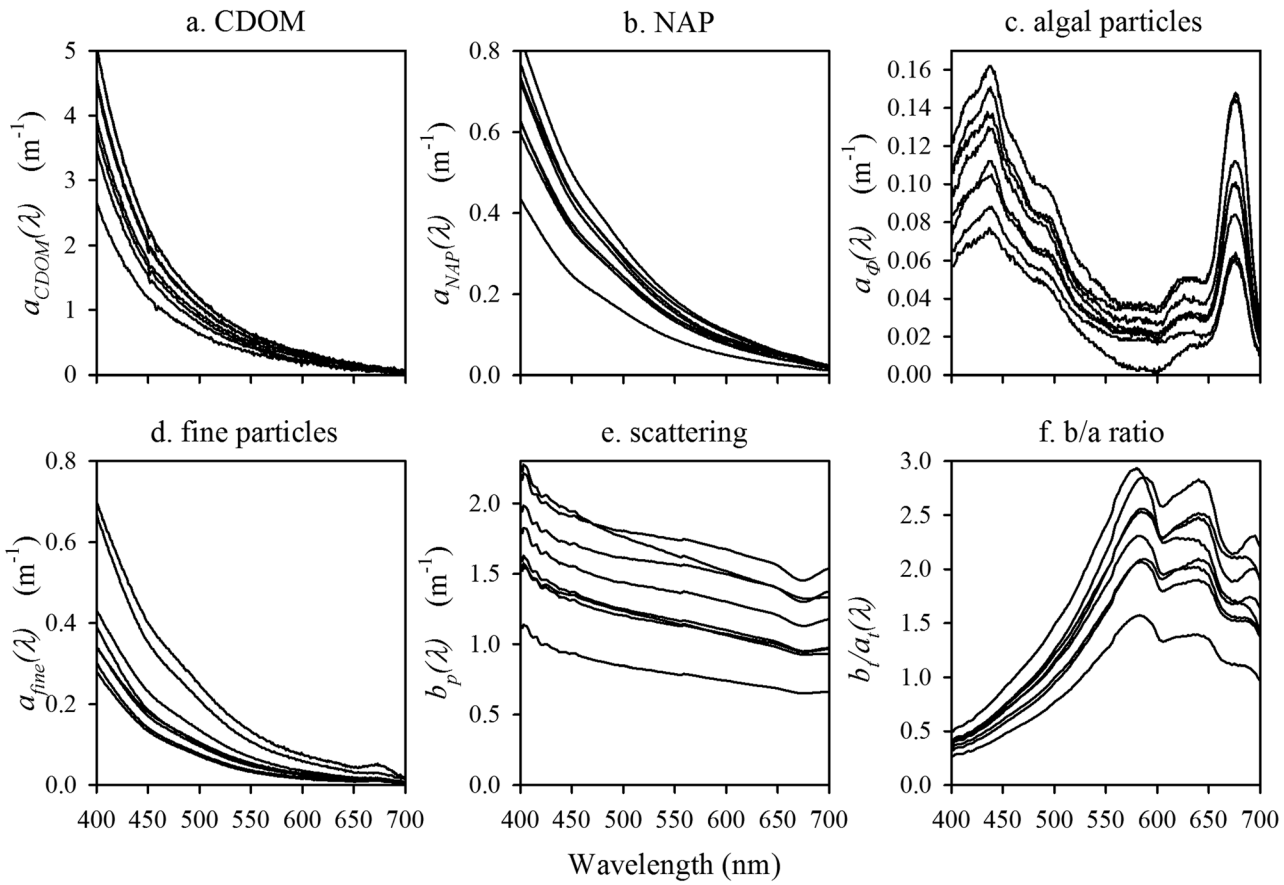

Figure 4. Spectral profiles of inherent optical properties: the absorption coefficients of (a) colored dissolved organic matter (CDOM), (b) nonalgal particulate matter (NAP), (c) algal particles, (d) fine particles, (e) the scattering coefficient of suspended particulate matter, and (f) the ratio of total scattering to total absorption coefficient (*b/a*). Observations are shown for all dates of sampling (n = 8).

Table 3. Summary of the Inherent Optical Properties Measured by a Laboratory Bench Top Spectrophotometer and a Wetlabs AC-S Spectrophometer: the Absorption Coefficients (*a*), Specific Absorption Coefficients (*a**), and Exponential Slope Parameters (*S*) for Absorbing Components: Colored Dissolved Organic Matter (CDOM), Nonalgal (NAP), Algal, and Fine Particles, the Scattering Coefficients of Suspended Particulate Matter (b_p), Specific Scattering Coefficients (b_p*), and the Ratios of Total Scattering to Total Absorption Coefficients (b_t/a_t)

	Optical Variable	Units	Range	Mean	CV (%)
CDOM	$a_{CDOM}(320)$	m^{-1}	9.92–18.77	15.30	19
	$a_{CDOM}(440)$	m^{-1}	1.38–2.65	2.16	20
	a_{CDOM}*(440)[a]	$m^2\ g^{-1}C$	0.560–0.690	0.624	6
	S_{CDOM}	nm^{-1}	0.0155–0.0158	0.0157	1
NAP	$a_{NAP}(440)$	m^{-1}	0.28–0.55	0.44	19
	a_{NAP}*(440)[a]	$m^2\ g^{-1}SPM$	0.190–0.259	0.219	13
	S_{NAP}	nm^{-1}	0.0096–0.0106	0.0101	4
Algal particles	$a_{\Phi}(440)$	m^{-1}	0.08–0.16	0.12	25
	$a_{\Phi}(660)$	m^{-1}	0.06–0.14	0.10	34
	a_{Φ}*(440)	$m^2\ mg^{-1}Chl\ a$	0.010–0.025	0.017	31
	a_{Φ}*(660)	$m^2\ mg^{-1}Chl\ a$	0.009–0.019	0.013	23
Fine particles	$a_{fine}(440)$	m^{-1}	0.16–0.45	0.26	43
Scattering	$b_p(440)$	m^{-1}	0.95–1.98	1.53	22
	$b_p(555)$	m^{-1}	0.78–1.74	1.31	24
	b_p*(440)	$m^2\ g^{-1}SPM$	0.635–0.870	0.760	13
	b_p*(555)	$m^2\ g^{-1}SPM$	0.537–0.755	0.652	13
b/a ratio	$b_t/a_t(440)$	dimensionless	0.407–0.781	0.588	19
	$b_t/a_t(585)$	dimensionless	1.57–2.88	2.35	19

[a]Data from 8 June were missing (n = 7).

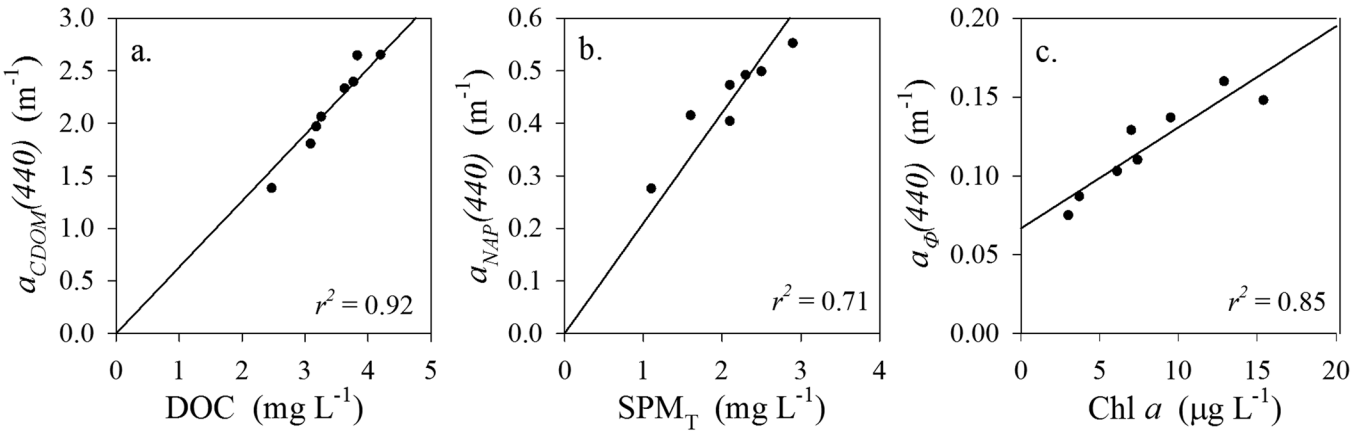

Figure 5. Relationship between (a) the absorption coefficients of colored dissolved organic matter at 440nm ($a_{CDOM}(440)$) and dissolved organic carbon (DOC); (b) the absorption coefficient of nonalgal particles at 440 nm ($a_{NAP}(440)$) and total suspended particulate matter (SPM_T); and (c) the absorption coefficient of algal particles at 440nm ($a_\Phi(440)$) and chlorophyll *a* concentrations (Chl *a*). Lines represent linear regression models (equations are given in the text).

The goodness-of-fit between measured and modeled irradiance was consistent across all dates of sampling (supporting information Figures S1 and S2), implying no major depth variations in IOPs throughout summer within the modeled surface layer, 0–6 m. However, there were large changes in the *in situ* absorption of PAR by the different optical constituents down the water column, as illustrated by the photon budget calculations for 19 September (Figure 8). The $a_{D;CDOM}(z;PAR)$ values (Figure 8a) decreased down the water column in parallel with $K_d(z;PAR)$, from 0.84 m^{-1} just below the surface to 0.25 m^{-1} at the bottom of the euphotic zone (4.3 m). Absorption by other nonwater absorbing components, NAP, algal particles, and fine particles also decreased with depth. For example, $a_{D;fine}(z;PAR)$ dropped over this depth range from 0.07 to 0.02 m^{-1}. In contrast, the *in situ* absorption by water molecules ($a_{D;w}(z;PAR)$) increased with depth, rising from 0.21 at the surface to 0.32 m^{-1} at the bottom of the euphotic zone, while $b_{b;D}(z;PAR)$ showed little vertical variation. At the top of the water column (just beneath the surface), the order of importance of each optical component in terms of % contribution to total photon attenuation was: CDOM (60%), water (15%), NAP (14%), fine particles (5%), algal particles (4%) and backscattering (2%). At the base of the euphotic zone, the order was: CDOM (43%), water (34%), NAP (12%), algal particles (6%), fine particles (3%), and backscattering (3%, sum is 101% due to rounding). These vertical characteristics and proportional contributions were consistent throughout the summer (Figure 9).

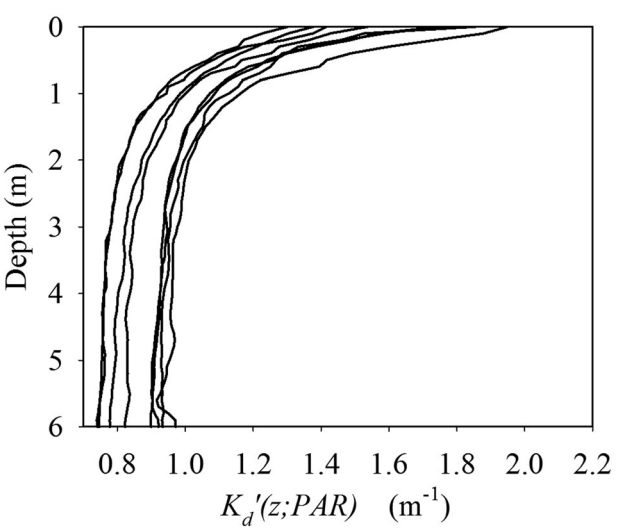

Figure 6. Vertical profiles of the estimated diffuse attenuation coefficient for PAR ($K_d'(z;PAR)$) for all eight sampling dates.

Seasonal variation in the estimated diffuse attenuation coefficient for PAR averaged over euphotic zone depth ($K_d'(z_{ave};PAR)$), just below the surface ($K'_d(0;PAR)$), and at the bottom of the euphotic zone ($K_d'(z_{eu};PAR)$) are shown in Figures 9a, 9c, and 9e, respectively. The seasonal trend for these variables was consistent with that of measured $K_d(PAR)$, with an increase from June to July followed by a gradual decrease throughout the summer. For the average over the euphotic zone, the range of $a_{D;CDOM}(z_{ave};PAR)$ was from 0.33 to 0.57 m^{-1}, and $a_{D;w}(z_{ave};PAR)$ from 0.25 to 0.31 m^{-1} (Table 4). Other components showed two to four-fold variations, but their absolute changes were smaller relative to those of CDOM and water (Table 4). There were close correlative relationships between the optical and

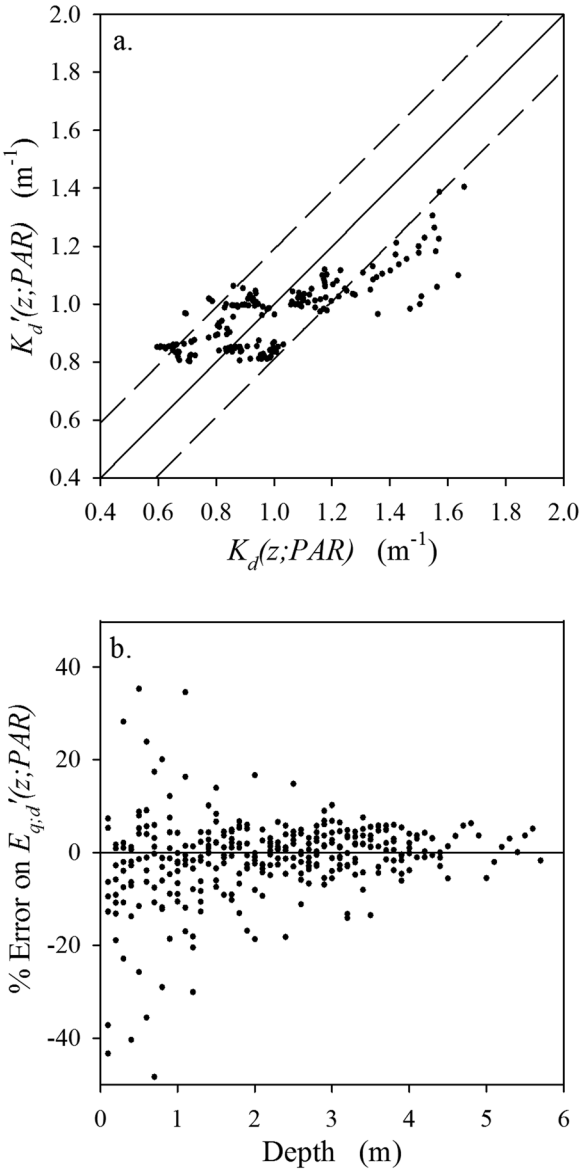

Figure 7. Comparison of photon budget calculations and measured values. (a) $K_d'(z;PAR)$ derived from the photon budget calculations versus $K_d(z;PAR)$ derived from log-linear regressions of measured photon flux density versus depth. The solid line indicates 1:1 relationship and the dashed lines show the range of root mean square error (±0.19 m^{-1}). (b) Percent error of estimated photon flux density relative to measured values as a function of depth. The solid line indicates zero % error.

limnological variables: $a_{D;CDOM}(z_{ave};PAR)$ versus DOC, $r = 0.97$ ($p < 0.01$); $a_{D;NAP}(z_{ave};PAR)$ versus SPM_T, $r = 0.92$ ($p < 0.01$); $a_{D;NAP}(z_{ave};PAR)$ versus SPM_I, $r = 0.88$ ($p = 0.01$); $a_{D;\Phi}(z_{ave};PAR)$ versus Chl *a*, $r = 0.95$ ($p < 0.01$); and $b_{b;D}(z_{ave};PAR)$ versus SPM_T, $r = 0.87$ ($p < 0.01$).

3.5. Photon Absorption Budget Calculations

The absorption analysis showed consistent dominance by CDOM in the absorption budget (Figure 9). For the observed range in limnological conditions, the contribution of algal pigments varied from 3 to 10% (Fig. 10), while that of CDOM varied from 32 to 55%. For extreme Chl *a* concentrations (50 μg L^{-1}) occurring in the condition where the concentrations of other components were at the minimum value of their observed ranges (DOC: 2.5 mg L^{-1}, SPM_T; 1.1 mg L^{-1}, $a_{fine}(440)$: 0.16 m^{-1}) the contribution of algal particles increased to 23%, but was still well below that of CDOM (38%).

4. Discussion

4.1. PAR Attenuation

On all dates of sampling, $K_d'(z;PAR)$ was highest at the surface and decreased with depth, due mostly to changes in the spectral distribution of $E_{q;d}(z;\lambda)$ down the water column. In the upper waters, there was higher diffuse absorption at shorter wavelengths. Deeper in the water column, PAR was depleted in shorter wavelength photons, and the remaining longer wavelength PAR was attenuated less strongly, resulting in lower values of $K_d'(z;PAR)$ at depth. This contrasts with oceanic systems [*Giles-Guzman and Alvarez-Borrego*, 2000; *Smith et al.*, 1989], in which $K_d'(z;PAR)$ also decreases with depth, but because of the attenuation of longer wavelength PAR in the surface waters and the shift to blue-dominated light at depth that is attenuated less by water itself. The decrease in $K_d(z;PAR)$ with depth is a universal phenomenon whenever the absorption spectrum ($a_t(\lambda)$) is uneven, and $K_d(z;PAR)$ will asymptotically approach the minimum value for $K_d(\lambda)$ as seen in this study, e.g., $K_d(z;PAR)$ reached 0.8 m^{-1} with depth (Figure 6), which is also the minimum value shown in Figure 3.

The component-specific coefficient profiles showed vertical changes due to the combined effects of their diffuse absorption and scattering characteristics and the spectral changes with depth (Figure 8). This effect is especially apparent in the estimates of per volume spectral diffuse absorption as a function of depth ($a_{D;i}(z;\lambda) \times E_{q;d}(z;\lambda)$, Figure 11). There were large vertical decreases in $a_{D;CDOM}(z;PAR)$, with more than a two-fold change from surface to the bottom of the euphotic zone. This change was associated with depletion of light at shorter wavelengths where CDOM has highest diffuse absorption. Similar vertical changes were

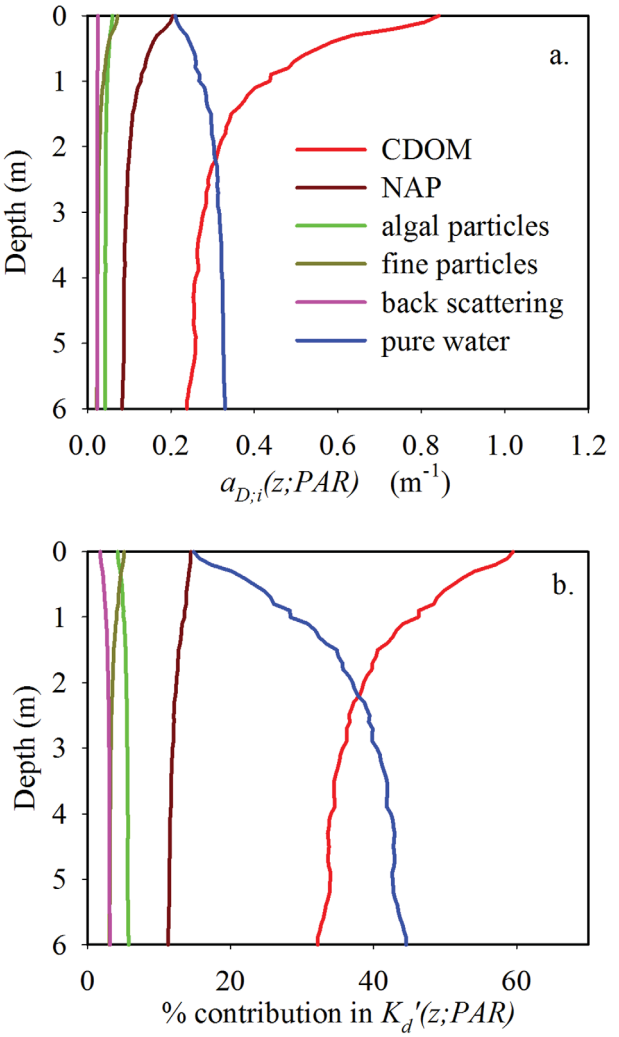

Figure 8. Vertical profiles of component-specific diffuse absorption/scattering coefficients for 19 September 2008: (a) absolute values and (b) proportional contribution to the total diffuse attenuation coefficient for PAR in %.

observed for both NAP and fine particles, components with similar exponential absorption curves as for CDOM. The diffuse absorption by algal particles also showed a depth-dependent decrease; however, it was smaller due to the bimodal shape of chlorophyll absorption spectra, with peaks in both the blue and red wavebands of the spectrum. Pure-water was the only component that showed a strong vertical increase, due to its higher absorption at longer wavelengths and the large absorption by CDOM in the upper water column that shifted the PAR spectrum toward these longer wavelengths. These vertical shifts in component-specific coefficient are universal when $K_d(PAR)$ is uneven over the spectrum. Backscattering showed little change down the water column because of its small spectral dependency.

The seasonal measurements of $K_d'(z;PAR)$ and its component structure indicate that variation in PAR attenuation of Lake St. Charles is mostly accounted for by changes in the diffuse absorption by CDOM (Figure 9), which in turn is a function of DOC concentration (see below). Other components showed two to four-fold seasonal variation in tandem with variations in their respective limnological variables; however, the ranges of variation and proportional contribution to total attenuation were small relative to those of CDOM. Algal particles, often considered to be the major controlling factor for underwater light and a commonly used indicator of lake water quality worldwide [e.g., *Dodson*, 2005; *Kalff*, 2002], made little contribution to PAR attenuation and its seasonal variability (Figures 9 and 11).

The importance of CDOM for PAR attenuation was reinforced by the photon absorption budget analysis which quantifies the fraction of incoming surface irradiance captured by each absorbing component (Figure 10). In the observed range of DOC concentrations during the study period (2.5–4.2 mg L^{-1}), CDOM maintained its dominance of PAR attenuation down the water column. Even when the conditions were under the combined influence of lowest DOC (2.5 mg L^{-1}) and extremely high Chl *a* concentrations (50 μg L^{-1}, extrapolated from observed data), CDOM still remained the primary absorbing component (29% compared to 20% for Chl *a*). These results indicate that CDOM is likely to be an important regulating factor of primary production in Lake St. Charles by competing with phototrophs for PAR, as in many coastal systems and inland waters elsewhere [*Karlsson et al.*, 2009; *Markager et al.*, 2004]. It also indicates that common optical measures of phytoplankton dynamics and water quality (e.g., radiometric determination of the diffuse attenuation coefficient for PAR and Secchi depth measurements of water column transparency) would be confounded in CDOM dominated water. Secchi depth is a function of not only $K_d(PAR)$ but also the beam attenuation coefficient for PAR ($c(PAR)$) [*Preisendorfer*, 1986], and the contribution of algal absorption to $c(PAR) + K_d(PAR)$ is even lower (average 3%). Although the contribution of algal particles to Secchi depth through scattering cannot be evaluated in the present data set, it should not exceed that of CDOM (average

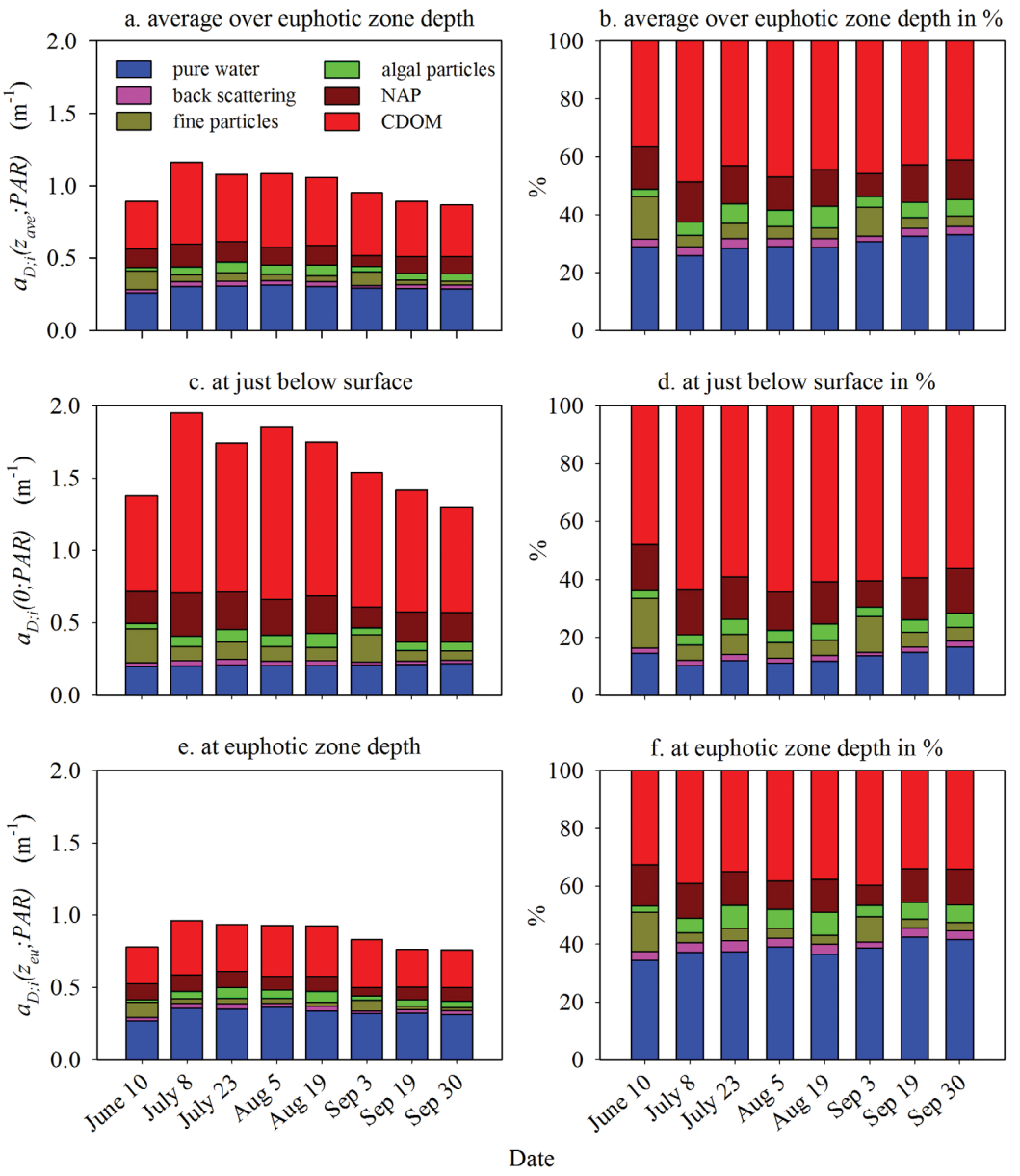

Figure 9. Seasonal changes in the contribution of each absorption component to the diffuse attenuation coefficient for PAR ($K_d'(z;PAR)$): (a) averaged over the euphotic zone, (c) just below the water surface, (e) at the bottom of the euphotic zone. (b, d, and f) The proportional contribution of each optical component to total $K_d'(z;PAR)$ in %.

31%). In Lake St. Charles, eutrophication accompanied with occasional cyanobacterial blooms have been a severe water quality concern in recent years, but Chl *a* concentrations in the pelagic zone rose to only 15 μg L^{-1} [*Rolland et al.*, 2013]. The present calculations show that this Chl *a* concentration would be poorly detected by standard water transparency measurements. Similar caution must be applied to lake monitoring practices throughout north temperate and boreal regions, where there are often large inputs of highly colored dissolved organic matter to lakes from their forested catchments [*Prairie et al.*, 2002].

4.2. The Photon Budget Analyses

The present study of PAR attenuation in Lake St. Charles combined field measurements of spectral irradiance with laboratory measurements of component-specific diffuse absorption and scattering spectra, and the photon budget calculations provided an improved understanding of the optical processes affecting underwater PAR attenuation. This type of spectral analysis has previously been limited to oceanic systems

Table 4. Summary of the Photon Budget Estimation: the Estimated Diffuse Attenuation Coefficient for PAR ($K_d'(z;PAR)$), the Diffuse Absorption Coefficients of Colored Dissolved Organic Matter ($a_{d;CDOM}(z_{ave};PAR)$), Nonalgal Particulate Matter ($a_{d;NAP}(z_{ave};PAR)$), Algal Particles ($a_{d;\Phi}(z_{ave};PAR)$), Fine Particles ($a_{d;Fine}(z_{ave};PAR)$), and Water ($a_{d;w}(z_{ave};PAR)$), the Diffuse Backscattering Coefficient ($b_{b;d}(z_{ave};PAR)$), and Their Percent Contribution to $K_d'(z;PAR)$

Factor	Range	Mean	CV (%)
$K_d'(z_{ave};PAR)$	0.87–1.16	1.00	10
$a_{D;CDOM}(z_{ave};PAR)$	0.33–0.57	0.44	18
$a_{D;NAP}(z_{ave};PAR)$	0.08–0.16	0.13	20
$a_{D;\Phi}(z_{ave};PAR)$	0.02–0.08	0.05	36
$a_{D;Fine}(z_{ave};PAR)$	0.03–0.13	0.06	58
$a_{D;w}(z_{ave};PAR)$	0.26–0.31	0.29	6
$b_{b;D}(z_{ave};PAR)$	0.02–0.04	0.03	24
$\%a_{D;CDOM}(z_{ave};PAR)$	37–49	44	8
$\%a_{D;NAP}(z_{ave};PAR)$	8–15	13	17
$\%a_{D;\Phi}(z_{ave};PAR)$	3–7	5	30
$\%a_{D;fine}(z_{ave};PAR)$	4–15	6	65
$\%a_{D;w}(z_{ave};PAR)$	26–33	30	8
$\%b_{b;D}(z_{ave};PAR)$	2–3	3	17

[*Giles-Guzman and Alvarez-Borrego*, 2000; *Smith et al*., 1989] and fjords [*Murray et al*., 2015]. The present study show that the photon budget approach is also useful for optically complex aquatic ecosystems where abiotic factors and phytoplankton may vary independently. This approach eliminates the need for complex radiative transfer modeling that requires a complete set of optical information for the water body [*Mobley*, 1994]. For example, the vertical profile of the CDOM-specific diffuse absorption coefficient down the water column can be obtained from the absorption coefficients of CDOM and downward irradiance profile, and such results can be applied to model photodegradation of dissolved organic matter [*Vähätalo and Wetzel*, 2004]. Similarly, other solar radiation-dependent processes in aquatic ecosystems can be modeled such as primary production [*Falkowski and Raven*, 2007; *Markager and Vincent*, 2001; *Morel*, 1991] and heat budgets [*Morel and Antoine*, 1994; *Patterson and Hamblin*, 1988]. This spectrally explicit approach is also increasingly attractive given that data sets from hyperspectral radiometers and advanced techniques for IOP analysis are becoming widely available.

The coupled AOP and IOP analysis applied here has several advantages over the estimation of component-specific attenuation coefficients by multiple linear regressions, as has been routinely applied to optically complex waters [e.g., *Carstensen et al*., 2013; *Duarte et al*., 1998; *Balogh et al*., 2009]. First, the photon budget approach provides detailed descriptions of the vertical gradient in spectral attenuation, while the more common regression approach provides only a water column averaged $K_d(PAR)$. Second, the estimations can be made with a single spectral irradiance profile and associated set of IOPs, and provide values specific to the site at the time of sampling. In contrast, the multiple linear regression approach requires a large number of observations, yet produces only a single averaged estimate that does not capture the large intra and inter-system variation in space and time. Third, the approach can be conducted even when optical components vary dependently. The optical components of natural waterbodies are not always independent (or weakly dependent) as in the present study, and multiple linear regressions, which require that explanatory variables are independent of each other, cannot be applied in such cases.

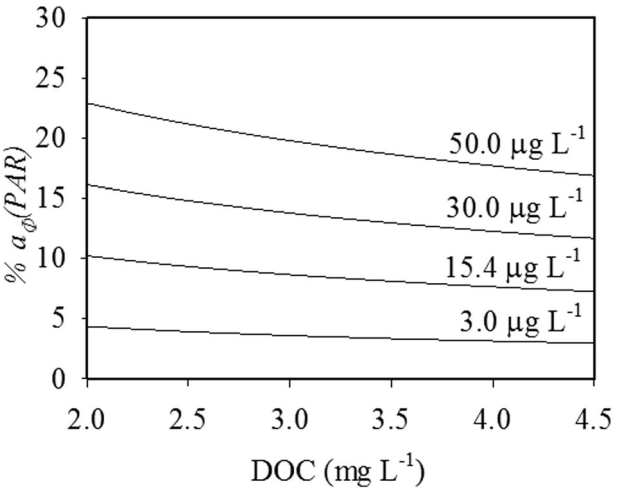

Figure 10. Photon absorption by phytoplankton (as a percentage of total absorption by all optical constituents) in relation to DOC concentration. The four curves are for different concentrations of Chl *a* (values in μg L^{-1}). The absorption by SPM_T and fine particles was maintained constant at the average measured values for Lake St. Charles.

Unlike the photon budget approach, multiple regression based analyses fail to take into account the spectral changes in the ambient light field, which can result in order of magnitude errors. For example, the diffuse absorption coefficient of pure-water for PAR has often been considered as a constant [*Morel*, 1988] given its fixed absorption spectrum [*Pope and Fry*, 1997]. However, as illustrated by the present study, the *in situ* diffuse absorption values for pure-water are subject to striking vertical and seasonal variations (Figure 8a and 9; Table 4), and $a_{D;w}(z;PAR)$ increased with depth on all dates of

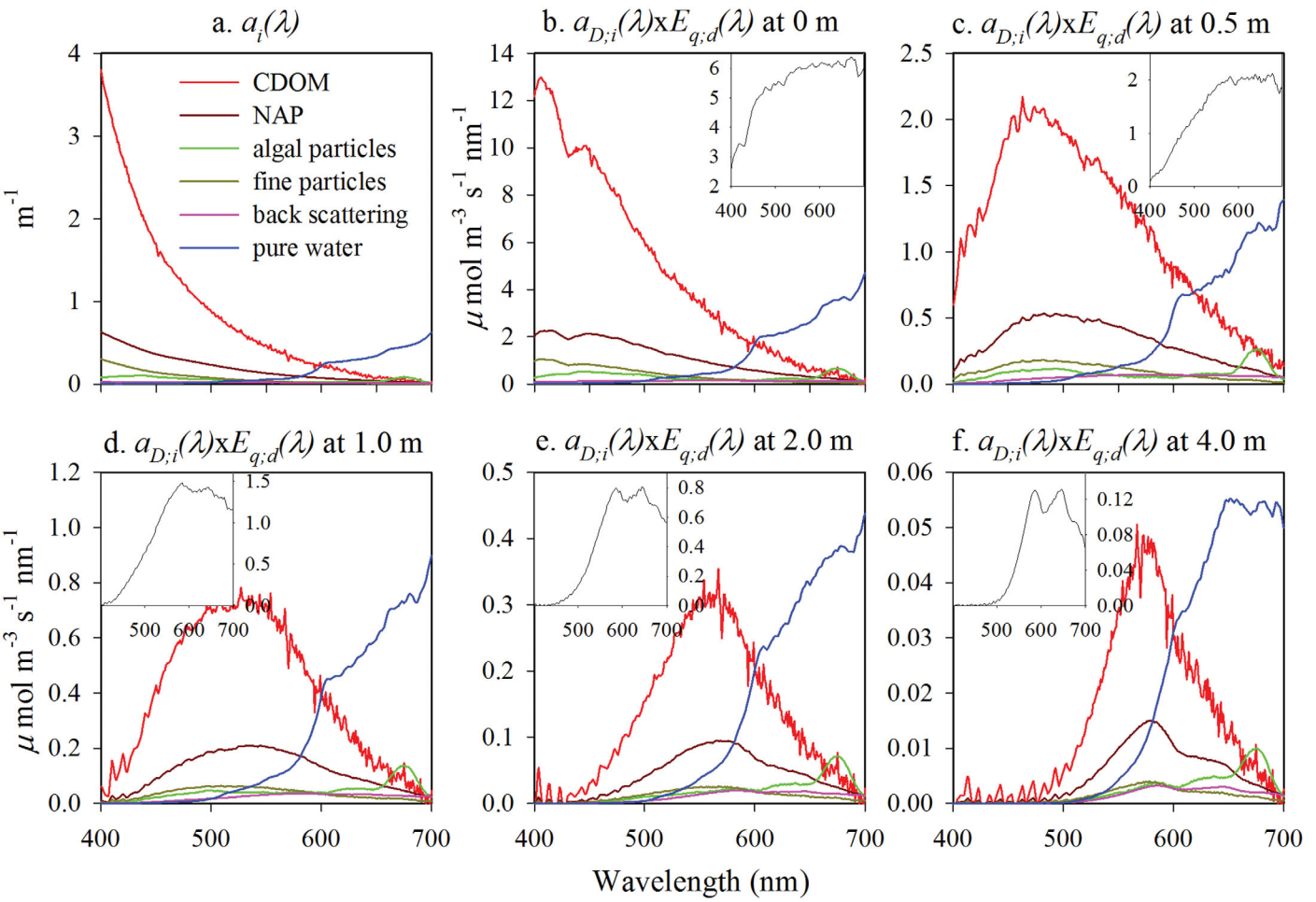

Figure 11. Spectra of the component-specific, volume absorption/scattering of photon flux ($a_{D;i}(z;\lambda) \times E_{q;d}(z;\lambda)$) at different depths down the water column, 19 September 2008: (a) Measurements of the inherent optical properties of the different optical components. (b–f) $a_{D;i}(z;\lambda) \times E_{q;d}(z;\lambda)$ at 0, 0.5, 1.0, 2.0, and 4.0 m, respectively; insert graphs: the measured $E_{q;d}(\lambda)$ spectrum at that depth.

sampling, in sharp contrast to diffuse absorption by the other optical components. This is also contrary to the pattern reported for oceanic systems, where *in situ* $a_{D;w}(z;PAR)$ decreases with depth because of the shift to bluer wavelengths [*Giles-Guzman and Alvarez-Borrego*, 2000; *Smith et al.*, 1989, *Murray et al.*, 2015]. The averaged $a_{D;w}(z;PAR)$ for the Lake St. Charles euphotic zone (0.29 m^{-1}, Table 4) was an order of magnitude higher than the classic values for oceanic Case 1 waters (0.027 m^{-1} [*Smith and Baker*, 1978]; 0.0384 m^{-1} [*Lorenzen*, 1972]), and which sometimes is applied in studies elsewhere, including Case 2 coastal and inland waters [e.g., *Obrador and Pretus*, 2008; *Balogh et al.*, 2009, and references therein]. This disparity between offshore marine and inland waters is the result of differences in spectral irradiance down their respective water columns.

In the present study, IOPs were measured in the surface water and were assumed to be constant throughout the water column. This is likely to be a source of error in the stratified period, as some vertical variation in the concentrations of optical components is known to occur in the lake. For example, *Bourget* [2011] reported that Chl *a* concentrations were higher in epilimnion relative to deeper in the water column. Such variation, however, would have little influence on our model results given the minor role of phytoplankton particles in PAR attenuation in this lake (Figures 9 and 11). Vertical variations in DOC would have a greater effect, given the dominant role of CDOM in PAR attenuation. DOC measured at 8 m was stable during sampled period (mean: 2.7 mg L^{-1}; range: 2.6–3.3 mg L^{-1}; CV: 9%), while that of surface water showed seasonal variability (Table 2). The mean difference between two depths ranged from −5 to 39% with a mean of 18%. Although the value was measured outside of either modeled

depth range (0–6 m) or euphotic zone depth (3.6–6 m), it gives some insight into DOC variability in hypolimnion. To assess the influence of such variations, we estimated $a_{CDOM}(\lambda)$ spectra from DOC at 8 m and applied it to the photon budget calculation (equation 7), assuming it to be the value in the hypolimnion. The mean absolute error on $K_d'(z;PAR)$ in hypolimnion ranged from 6 to 23% (mean 16%). The error on average percent contribution of optical components for euphotic zone as shown on Figure 9b was minor except for 8 July when the contribution of CDOM decreased (from 47 to 37%) and that of water increased (from 28 to 33%), with little change in the percent contribution of the other components. We further evaluated the potential effects of variable DOC down the water column using HydroLight, and this confirmed that large depth variations in DOC would lead to pronounced changes in $K_d'(z;PAR)$ (see supporting information Figure S3).

Despite the potential sources of error discussed above, there were no major discrepancies in the model validation, except for the observations taken near the water surface ($<$ 2m) where the measurement error on irradiance profile was large due to natural variation of light field, likely induced by wave motion (Figure 7b). For future studies, the application of IOP profiles taken by an *in situ* spectrophotometer (such as casts of the AC meter with and without 0.2 μm membrane filters to measure CDOM and particulate absorption profiles) or of fluorometric measurements of CDOM and Chl *a* may be useful to obtain improved estimates of variation down the water column, and these could be easily incorporated in the photon budget calculations for $K_d'(z;PAR)$.

4.3. Optical Components

The observed high $a_{CDOM}^*(\lambda)$ and low S_{CDOM} values imply that dissolved organic matter in Lake St. Charles is highly colored [*Morris et al*., 1995; *Stedmon et al*., 2000]. Also, the muted seasonal variations in these variables suggest that there was little qualitative variation throughout the summer, and that seasonal changes in CDOM absorption were almost entirely due to shifts in the concentration of dissolved organic matter. This carbon pool may be dominated by terrigenous carbon from catchments mostly covered by deciduous forests [*Pienitz and Vincent*, 2003; *Tremblay et al*., 2001]. The influence of photochemical or biological degradation, which is known to cause seasonal changes in the optical properties of CDOM [*Vähätalo and Wetzel*, 2004], may be minimal due to the relatively high hydraulic flushing rate in this lake (72 days) [*Rolland et al*., 2013], as in many drinking water reservoirs. This qualitative stability in the carbon pool and strong linearity in the CDOM-DOC relationship implies that CDOM absorption can serve as an index to estimate DOC concentrations in Lake St. Charles, and vice versa. Similarly strong relationships have been found in other water bodies [*Stedmon et al*., 2006]; however, this estimation would be feasible only within a water body, given that $a_{CDOM}^*(\lambda)$ may vary significantly between systems [*Watanabe et al*., 2009].

The $a_{NAP}^*(440)$ values in the lake (mean 0.219 $m^2\ g^{-1}$) were considerably higher than previously reported for other aquatic systems [*Babin et al*., 2003b; *Belzile et al*., 2004; *Binding et al*., 2008]. This high mass-specific absorption may be the combined result of the NAP particle size distribution dominated by smaller particles, and the particle composition, with a higher proportion of mineral rich particles [*Babin et al*., 2003b; *Binding et al*., 2008; *Stramski et al*., 2007]. Adsorption of highly colored CDOM to these nonalgal particles could also contribute to higher mass-specific absorption, although this effect cannot be evaluated from the present data set. The coefficient $a_{NAP}(\lambda)$ is assumed to describe the absorption by both inorganic and organic component of nonalgal particles, while SPM_T incorporates the dry weight of algal particles in addition to nonalgal components. Also, SPM_I is assumed to be exclusively composed of the inorganic portion of nonalgal particles. This difference between the absorption and dry weight measurements may confound interpretation of the mass-specific absorption estimates. Despite this uncertainty, however, the small variations observed in $a_{NAP}^*(440)$ and S_{NAP}, and the strong $a_{NAP}(440)$-SPM_T and $a_{NAP}(440)$-SPM_I relationships, indicate that the optical characteristics of NAP were relatively stable over the sampling period, and that variation in $a_{NAP}(440)$ was largely the result of changes in concentration of suspended particles. This characteristic means that it would be feasible to estimate suspended particle concentrations from optical data, and conversely to apply SPM measurements in combination with the $a_{NAP}^*(\lambda)$ for the forward modeling of AOPs of the lake.

The two-fold variations in algal absorption were well explained by the changes in Chl *a* concentration in the lake, and the Chl *a*-specific absorption values fell within the range reported elsewhere [*Bricaud et al*., 1995; *Dekker et al*., 2002; *Zhang et al*., 2010]. These characteristics suggest that estimation of algal absorption

spectra from Chl *a* concentrations and subsequent modeling of primary production [*Falkowski and Raven*, 2007; *Morel*, 1991] may be feasible in this lake. However, the remote observation of Chl *a* in this and similar lakes with moderate or higher CDOM concentrations will require careful optical analysis given that the contribution of algal absorption to overall PAR attenuation is low compared to other optical components (Figures 8 and 9), and that these other components (CDOM and NAP) are not statistically correlated, unlike in open ocean waters.

Fine particles are defined as particulate matter passing through glass fiber filters (Whatman GF/F in the present study) but caught on membrane filters with a pore size of 0.2 μm (Millipore nitrocellulose membrane filters in the present study). Particles in this size fraction have been commonly observed in a variety of highly turbid systems such as reservoirs in agricultural areas [*Jones et al*., 2008], thaw ponds in subarctic discontinuous permafrost [*Watanabe et al*., 2011], and the estuary of a large river [*Gallegos*, 2005]. In certain systems, they can be an important optical component [*Gallegos*, 2005; *Watanabe et al*., 2011]. To our knowledge, however, they have not previously been considered in low turbidity inland waters such as the reservoir sampled here, and their detailed optical properties have been little explored. In the present study, the absorption by fine particles was detected throughout the summer. Although their absorption was lower relative to CDOM absorption, it was equivalent to NAP absorption at times (Figure 4). This suggests that fine particles may exert a significant influence on optical processes, not only in highly turbid systems but also in mesotrophic waters, and their light absorbing and scattering properties require much closer attention.

The fine particles in the lake had exponentially shaped absorption spectra with a small peak at 680 nm (Figure 4d) implying that they were mostly nonalgal with only a minor contribution of phytoplankton. The proportional contribution of these particles to total particulate absorption may vary seasonally. On two sampling dates, there were relatively higher fine particle absorption values (Figure 4d). The early summer observation ($a_{fine}(440) = 0.45$ m^{-1}, 10 June) showed a clear peak at 680 nm, indicating a significant contribution by phytoplankton pigments. On the other hand, the mid-summer curve ($a_{fine}(440) = 0.40$ m^{-1}, 3 September) showed no such peak, suggesting a lower algal contribution to absorption at that time. This difference illustrates the compositional shifts in fine particles through time.

The shapes of the $b_p(\lambda)$ spectra were consistent throughout the summer, except for the one observation showing a steeper curve (8 July, Figure 4e). Although differences in particle composition or size distribution may produce such a deviation [*Babin et al*., 2003a; *Twardowski et al*., 2001], characterization of the spectra by a power model exponent [*Babin et al*., 2003a; *Belzile et al*., 2004] was not possible for the present data set due to the influence of algal pigment absorption. Thus, estimation of spectra for forward modeling [*Mobley*, 1994] by applying the power model would not be appropriate. However, the relatively consistent spectral shape and the strong linear relationship between $b_p(\lambda)$ and SPM_T may allow the estimation of SPM_T from $b_p(\lambda)$, and the application of SPM_T for forward modeling of AOPs in a manner analogous to that for NAP absorption.

Our results imply that $b_{b;D}(z;PAR)$ can be omitted from the $K_d'(z;PAR)$ estimation if information regarding scattering is not available. In the present study, the contribution of the $b_{b;D}(z;PAR)$ to $K_d'(z;PAR)$ was always less than four percent in the entire water column throughout the summer (Figures 8 and 9); thus, removal of $b_{b;D}(z;PAR)$ from equation (8) would only cause minor underestimation of $K_d'(z;PAR)$. However, both application of a constant backscattering ratio and removal of $b_{b;D}(z;PAR)$ from the estimation should be carefully examined in more turbid systems where scattering makes a greater contribution to PAR attenuation.

5. Conclusions

The photon budget analysis applied in the present study provides a simplified approach toward partitioning underwater PAR attenuation into its spectral absorption and scattering components, and their variations with depth. This analysis showed that for Lake St. Charles, a northern temperate reservoir subject to harmful algal blooms, PAR attenuation was dominated by CDOM absorption. Phytoplankton had a minimal influence on spectral attenuation and water transparency, except at simulated chlorophyll *a* values that were well above those observed during blooms in the lake. These optical conditions limit the application of traditional water quality descriptors such as radiometric transparency and Secchi depth in DOC-colored lakes and reservoirs.

Acknowledgments
This project was funded by the Natural Sciences and Engineering Research Council and the Canada Research Chair program. We thank E. Boss for critically reviewing the draft manuscript, M. Babin for valuable discussions, and S. Bourget, M.-J. Martineau, R. Tremblay, G. Sarasin, M.-A. Couillard, and D. Rolland for their assistance in the field and laboratory. Results displayed in figures or tables in this article can be obtained from the lead author.

References

APHA (1998), *Standard Methods for Examination of Water and Wasterwater*, 20th ed., 1325 pp., Am. Public Health Assoc., Washington, D. C.

Babin, M., and D. Stramski (2002), Light absorption by aquatic particles in the near-infrared spectral region, *Limnol. Oceanogr.*, *47*(3), 911–915.

Babin, M., A. Morel, V. Fournier-Sicre, F. Fell, and D. Stramski (2003a), Light scattering properties of marine particles in coastal and open ocean waters as related to the particle mass concentration, *Limnol. Oceanogr. Methods*, *48*(2), 843–859.

Babin, M., D. Stramski, G. M. Ferrari, H. Claustre, A. Bricaud, G. Obolensky, and N. Hoepffner (2003b), Variations in the light absorption coefficients of phytoplankton, nonalgal particles, and dissolved organic matter in coastal waters around Europe, *J. Geophys. Res.*, *108*(C7), 3211, doi:10.1029/2001JC000882.

Balogh, K. V., B. Nemeth, and L. Voros (2009), Specific attenuation coefficients of optically active substances and their contribution to the underwater ultraviolet and visible light climate in shallow lakes and ponds, *Hydrobiologia*, *632*(1), 91–105.

Belzile, C., W. F. Vincent, C. Howard-Williams, I. Hawes, M. James, M. Kumagai, and C. Roesler (2004), Relationships between spectral optical properties and optically active substances in a clear oligotrophic lake, *Water Resour. Res.*, *40*, W12512, doi:10.1029/2004WR003090.

Berwald, J., D. Stramski, C. D. Mobley, and D. A. Kiefer (1995), Influences of absorption and scattering on vertical changes in the average cosine of the underwater light field, *Limnol. Oceanogr.*, *40*(8), 1347–1357.

Binding, C. E., J. H. Jerome, R. P. Bukata, and W. G. Booty (2008), Spectral absorption properties of dissolved and particulate matter in Lake Erie, *Remote Sens. Environ.*, *112*(4), 1702–1711.

Boss, E., W. S. Pegau, M. Lee, M. Twardowski, E. Shybanov, G. Korotaev, and F. Baratange (2004), Particulate backscattering ratio at LEO 15 and its use to study particle composition and distribution, *J. Geophys. Res.*, *109*, C01014, doi:10.1029/2002JC001514.

Bourget, S. (2011), *Limnologie et charge en phosphore d'un réservoir d'eau potable sujet à des fleurs d' eau de cyanobactéries : Le Lac Saint-Charles, Québec*, 144 pp., Univ. Laval, Québec, Canada.

Boyce, D. G., M. R. Lewis, and B. Worm (2010), Global phytoplankton decline over the past century, *Nature*, *466*(7306), 591–596.

Breton, J., C. Vallieres, and I. Laurion. (2009), Limnological properties of permafrost thaw ponds in northeastern Canada, *Can. J. Fish. Aquat. Sci.*, *66*, 1635–1648.

Bricaud, A., and D. Stramski (1990), Spectral absorption-coefficients of living phytoplankton and nonalgal biogenous matter—A comparison between the Peru upwelling area and the Sargasso Sea, *Limnol. Oceanogr.*, *35*(3), 562–582.

Bricaud, A., A. Morel, and L. Prieur (1981), Absorption by dissolved organic-matter of the sea (yellow substance) in the UV and visible domains, *Limnol. Oceanogr.*, *26*(1), 43–53.

Bricaud, A., M. Babin, A. Morel, and H. Claustre (1995), Variability in the chlorophyll-specific absorption-coefficients of natural phytoplankton—Analysis and parameterization, *J. Geophys. Res.*, *100*(C7), 13,321–13,332.

Buiteveld, H., J. H. M. Hakvoort, and M. Donze (1994), The optical properties of pure water, *Proc. SPIE*, *2258*, 174–183.

Bukata, R. P. (2005), *Satellite Monitoring of Inland and Coastal Water Quality: Retrospection, Introspection, Future Directions*, 272 pp., Taylor & Francis/CRC Press, U. K.

Carstensen, J., D. Krause-Jensen, S. Markager, K. Timmermann, and J. Windolf (2013), Water clarity and eelgrass responses to nitrogen reductions in the eutrophic Skive Fjord, Denmark, *Hydrobiologia*, *704*(1), 293–309.

Cleveland, J. S., and A. D. Weidemann (1993), Quantifying absorption by aquatic particles—A multiple-scattering correction for glass-fiber filters, *Limnol. Oceanogr.*, *38*(6), 1321–1327.

Dekker, A. G., R. J. Vos, and S. W. M. Peters (2002), Analytical algorithms for lake water TSM estimation for retrospective analyses of TM and SPOT sensor data, *Int. J. Remote Sens.*, *23*(1), 15–35.

Dodson, S. (2005), *Introduction to Limnology*, 400 pp., McGraw-Hill, N. Y.

Duarte, C. M., S. Agusti, M. P. Satta, and D. Vaque (1998), Partitioning particulate light absorption: A budget for a Mediterranean bay, *Limnol. Oceanogr.*, *43*(2), 236–244.

Falkowski, P., and J. Raven (2007), *Aquatic Photosynthesis*, 2nd ed., 484 pp., Princeton Univ. Press, Princeton, N. J.

Ferrari, G. M., and S. Tassan (1996), Use of the 0.22 μm Millipore membrane for light-transmission measurements of aquatic particles, *J. Plankton Res.*, *18*(7), 1261–1267.

Gallegos, C. L. (2005), Optical water quality of a blackwater river estuary: The Lower St. Johns River, Florida, USA, *Estuarine Coastal Shelf Sci.*, *63*(1-2), 57–72.

Gallegos, C. L., R. J. Davies-Colley, and M. Gall (2008), Optical closure in lakes with contrasting extremes of reflectance, *Limnol. Oceanogr. Methods*, *53*(5), 2021–2034.

Giles-Guzman, A. D., and S. Alvarez-Borrego (2000), Vertical attenuation coefficient of photosynthetically active radiation as a function of chlorophyll concentration and depth in case 1 waters, *Appl. Opt.*, *39*(9), 1351–1358.

International Ocean Color Coordinating Group (IOCCG) (2000), *Remote Sensing of Ocean Colour in Coastal, and Optically-Complex, Waters*, 140 pp., Dartmouth, Nova Scotia, Canada.

Jones, J. R., D. V. Obrecht, B. D. Perkins, M. F. Knowlton, A. P. Thorpe, S. Watanabe, and R. R. Bacon (2008), Nutrients, seston, and transparency of Missouri reservoirs and oxbow lakes: An analysis of regional limnology, *Lake Reservoir Manage.*, *24*(2), 155–180.

Kalff, J. (2002), *Limnology: Inland Water Ecosystems*, 592 pp., Prentice Hall, Upper Saddle River, N. J.

Karlsson, J., P. Bystrom, J. Ask, P. Ask, L. Persson, and M. Jansson (2009), Light limitation of nutrient-poor lake ecosystems, *Nature*, *460*(7254), 506–509.

Kirk, J. T. O. (1981), Monte Carlo study of the nature of the underwater light field in, and the relationships between optical properties of, turbid yellow waters, *Aust. J. Mar. Fresh. Res.*, *32*(4), 517–532.

Kirk, J. T. O. (1994), *Light and Photosynthesis in Aquatic Ecosystems*, 2nd ed., 509 pp., Cambridge Univ. Press, Cambridge, U. K.

Kishino, M., M. Takahashi, N. Okami, and S. Ichimura (1985), Estimation of the spectral absorption-coefficients of phytoplankton in the sea, *Bull. Mar. Sci.*, *37*(2), 634–642.

Koenings, J. P., and J. A. Edmundson (1991), Secchi disk and photometer estimates of light regimes in Alaskan lakes—Effects of yellow color and turbidity, *Limnol. Oceanogr.*, *36*(1), 91–105.

Loisel, H., X. Meriaux, J. F. Berthon, and A. Poteau (2007), Investigation of the optical backscattering to scattering ratio of marine particles in relation to their biogeochemical composition in the eastern English Channel and southern North Sea, *Limnol. Oceanogr. Methods*, *52*(2), 739–752.

Lorenzen, C. J. (1972), Extinction of light in the ocean by phytoplankton, *J. Cons. Cons. Int. Explor. Mer.*, *32*(2), 262–267.

Markager, S. and K. Sand-Jensen (1992), Light requirements and depth zonation of marineacroalgae, *Mar. Ecol. Prog. Ser.*, *88*, 83–92.

Markager, S., and W. F. Vincent (2001), Light absorption by phytoplankton: Development of a matching parameter for algal photosynthesis under different spectral regimes, *J. Plankton Res.*, *23*(12), 1373–1384.
Markager, S., C. A. Stedmon, and P. Conan (2004), Effects of DOM in marine ecosystems, in *Dissolved Organic Matter (DOM) in Aquatic Ecosystems: A Study of European Catchments and Coastal Waters*, edited by M. Søndergaard and D. N. Thomas, pp. 37–42, EU project DOMAINE, Hillerød, Denmark.
MDDEP (2007), *Méthodes du Réseau de surveillance volontaire des lacs de villégiature*, Minist. du Dév. durable, de l'Environnement et des Parcs du Québec, Quebec, Canada. [Available at http://www.mddelcc.gouv.qc.ca/eau/rsvl/.]
Middelboe, A. and S. Markager (1997), Depth limits and minimum light requirements of freshwater macrophytes, *Freshwater Biol.*, *37*, 553–568.
Mitchell, B. G., et al. (2000), Determination of spectral absorption coefficients of particles, dissolved material and phytoplankton for discrete water samples, in *Ocean Optics Protocols for Satellite Ocean Color Sensor Validation, Revision 2*, edited by G. S. Fargion and J. L. Mueller, pp. 125–153, Natl. Aeronauti. and Space Admin., Greenbelt, Md.
Mitchell, B. G., M. Kahru, J. Wieland, and M. Stramska (2002), Determination of spectral absorption coefficients of particles, dissolved material and phytoplankton for discrete water samples, in *Ocean Optics Protocols for Satellite Ocean Color Sensor Validation, Revision 4*, edited by J. L. Mueller and G. S. Fargion, pp. 39–64, Natl. Aeronaut. and Space Admin., Greenbelt, Md.
Mobley, C. D. (1994), *Light and Water: Radiative Transfer in Natural Waters*, 592 pp., Academic, San Diego, Calif.
Morel, A. (1988), Optical modeling of the upper ocean in relation to its biogenous matter content (Case-I waters), *J. Geophys. Res.*, *93*(C9), 10,749–10,768.
Morel, A. (1991), Light and marine photosynthesis—A spectral model with geochemical and climatological implications, *Prog. Oceanogr.*, *26*(3), 263–306.
Morel, A., and D. Antoine (1994), Heating rate within the upper ocean in relation to its biooptical state, *J. Phys. Oceanogr.*, *24*(7), 1652–1665.
Morris, D. P., H. Zagarese, C. E. Williamson, E. G. Balseiro, B. R. Hargreaves, B. Modenutti, R. Moeller, and C. Queimalinos (1995), The attentuation of solar UV radiation in lakes and the role of dissolved organic carbon, *Limnol. Oceanogr.*, *40*(8), 1381–1391.
Murray, C., S. Markager, C. A. Stedmon, T. Juul-Pedersen, M. Sejr, and A. Bruhn (2015), The influence of glacial meltwater on bio-optical properties in two contrasting Greenland fjords, *Estuarine and Coastal Shelf Science*, *163*, 72–83, doi:10.1016/j.ecss.2015.05.041.
Nusch, E. A. (1980), Comparison of different methods for chlorophyll and phaeopigment determination, *Arch. Hydrobiol.*, *14*, 14–36.
Obrador, B., and J. L. Pretus (2008), Light regime and components of turbidity in a Mediterranean coastal lagoon, *Estuarine Coastal Shelf Sci.*, *77*(1), 123–133.
Patterson, J. C., and P. F. Hamblin (1988), Thermal simulation of a lake with winter ice cover, *Limnol. Oceanogr.*, *33*(3), 323–338.
Pegau, S., J. R. V. Zaneveld, B. G. Mitchell, J. L. Mueller, M. Kahru, J. Wieland, and M. Stramska (2003), Inherent optical properties: Instruments, characterizations, field measurements and data analysis protocols, in *Ocean optics protocols for satellite ocean color sensor validation; Revision 4*, edited by J. L. Mueller, G. S. Fargion and R. McClain, Natl. Aeronaut. and Space Admin., Greenbelt, Md.
Peng, F., S. W. Effler, D. O'Donnell, A. D. Weidemann, and M. T. Auer (2009), Characterizations of minerogenic particles in support of modeling light scattering in Lake Superior through a two-component approach, *Limnol. Oceanogr. Methods*, *54*(4), 1369–1381.
Petzold, T. J. (1972), Volume scattering functions for selected ocean waters, *Rep. SIO 72–78*, Scripps Inst. of Oceanogr., San Diego, Calif.
Pienitz, R., and W. F. Vincent (2003), Generic approaches towards water quality monitoring based on Paleolimnology, in *Freshwater Management—Global versus Local Perspectives*, edited by M. Kumagai and W. F. Vincent, pp. 61–82, Springer, Tokyo.
Pope, R. M., and E. S. Fry (1997), Absorption spectrum (380–700 nm) of pure water .2. Integrating cavity measurements, *Appl. Opt.*, *36*(33), 8710–8723.
Prairie, Y. T., D. F. Bird, and J. J. Cole (2002), The summer metabolic balance in the epilimnion of southeastern Quebec lakes, *Limnol. Oceanogr.*, *47*(1), 316–321.
Preisendorfer, R. W. (1961), *Application of Radiative Transfer Theory to Light Measurements in the Sea, Union Geod. Geophys. Int. Monogr.*, vol. 10, pp. 11–30.
Preisendorfer, R. W. (1976), *Hydrologic Optics*, NOAA Pac. Mar. Environ. Lab., Seattle, Wash.
Preisendorfer, R. W. (1986), Secchi Disk Science—Visual Optics of Natural-Waters, *Limnol. Oceanogr.*, *31*(5), 909–926.
R Development Core Team (2013), *R: A Language and Environment for Statistical Computing Version 3.0.1*, R Found. for Stat. Comput., Vienna, Austria.
Roesler, C. S. (1998), Theoretical and experimental approaches to improve the accuracy of particulate absorption coefficients derived from the quantitative filter technique, *Limnol. Oceanogr.*, *43*(7), 1649–1660.
Rolland, D. C., and W. F. Vincent (2014), Characterization of phytoplankton seed banks in the sediments of a drinking water reservoir, *Lake Reservoir Manage.*, *30*(4), 371–380.
Rolland, D. C., S. Bourget, A. Warren, I. Laurion, and W. F. Vincent (2013), Extreme variability of cyanobacterial blooms in an urban drinking water supply, *J. Plankton Res.*, *35*(4), 744–758.
Smith, R. C., and K. S. Baker (1978), The bio-optical state of ocean waters and remote sensing, *Limnol. Oceanogr.*, *23*(2), 247–259.
Smith, R. C., J. Marra, M. J. Perry, K. S. Baker, E. Swift, E. Buskey, and D. A. Kiefer (1989), Estimation of a photon budget for the upper ocean in the Sargasso sea, *Limnol. Oceanogr.*, *34*(8), 1673–1693.
Stavn, R. H. (1988), Lambert-Beer law in ocean waters–Optical properties of water and of dissolved/suspended material, optical energy budgets, *Appl. Opt.*, *27*(2), 222–231.
Stedmon, C. A., S. Markager, and H. Kaas (2000), Optical properties and signatures of chromophoric dissolved organic matter (CDOM) in Danish coastal waters, *Estuarine Coastal Shelf Sci.*, *51*(2), 267–278.
Stedmon, C. A., S. Markager, M. Sondergaard, T. Vang, A. Laubel, N. H. Borch, and A. Windelin (2006), Dissolved organic matter (DOM) export to a temperate estuary: Seasonal variations and implications of land use, *Estuaries Coasts*, *29*(3), 388–400.
Stramski, D., M. Babin, and S. B. Wozniak (2007), Variations in the optical properties of terrigenous mineral-rich particulate matter suspended in seawater, *Limnol. Oceanogr. Methods*, *52*(6), 2418–2433.
Sullivan, J. M., M. S. Twardowski, J. R. V. Zaneveld, C. M. Moore, A. H. Barnard, P. L. Donaghay, and B. Rhoades (2006), Hyperspectral temperature and salt dependencies of absorption by water and heavy water in the 400–750 nm spectral range, *Appl. Opt.*, *45*(21), 5294–5309.
Tremblay, R., S. Légaré, R. Pienitz, W. F. Vincent, and R. Hall (2001), Étude paléolimnologique de l'histoire trophique du lac Saint-Charles, réservoir d'eau potable de la communauté urbaine de Québec, *Rev. Sci. Eau.*, *14*(4), 489–510.
Twardowski, M. S., J. M. Sullivan, P. L. Donaghay, and J. R. V. Zaneveld (1999), Microscale quantification of the absorption by dissolved and particulate material in coastal waters with an ac-9, *J. Atmos. Ocean. Technol.*, *16*(6), 691–707.
Twardowski, M. S., Boss, E., Macdonald, J. B., Pegau, W. S., Barnard, A. H., & Zaneveld, J. R. V. (2001), A model for estimating bulk refractive index from the optical backscattering ratio and the implications for understanding particle composition in case I and case II waters, *J. Geophys. Res.*, *106*(C7), 14,129–14,142.

Vähätalo, A. V., and R. G. Wetzel (2004), Photochemical and microbial decomposition of chromophoric dissolved organic matter during long (months-years) exposures, *Mar. Chem.*, *89*(1-4), 313–326.

Watanabe, S., M. F. Knowlton, W. F. Vincent, and J. R. Jones (2009), Variability in the optical properties of colored dissolved organic matter in Missouri reservoirs, *Verh. Int. Verein. Limnol.*, *30*(7), 1117–1120.

Watanabe, S., I. Laurion, K. Chokmani, R. Pienitz, and W. F. Vincent (2011), Optical diversity of thaw ponds in discontinuous permafrost: A model system for water color analysis, *J. Geophys. Res.*, *116*, G02003, doi:10.1029/2010JG001380.

Zhang, Y. L., L. Q. Feng, J. S. Li, L. C. Luo, Y. Yin, M. L. Liu, and Y. L. Li (2010), Seasonal-spatial variation and remote sensing of phytoplankton absorption in Lake Taihu, a large eutrophic and shallow lake in China, *J. Plankton Res.*, *32*(7), 1023–1037.